Title
Intestinal Snakeskin Limits Microbial Dysbiosis during Aging and Promotes Longevity

Authors
Salazar, Anna M
Resnik-Docampo, Martin
Ulgherait, Matthew
et al.

Publication Date
2018-11-01

DOI
10.1016/j.isci.2018.10.022

Peer reviewed

iScience

CellPress

Article

Intestinal Snakeskin Limits Microbial Dysbiosis during Aging and Promotes Longevity

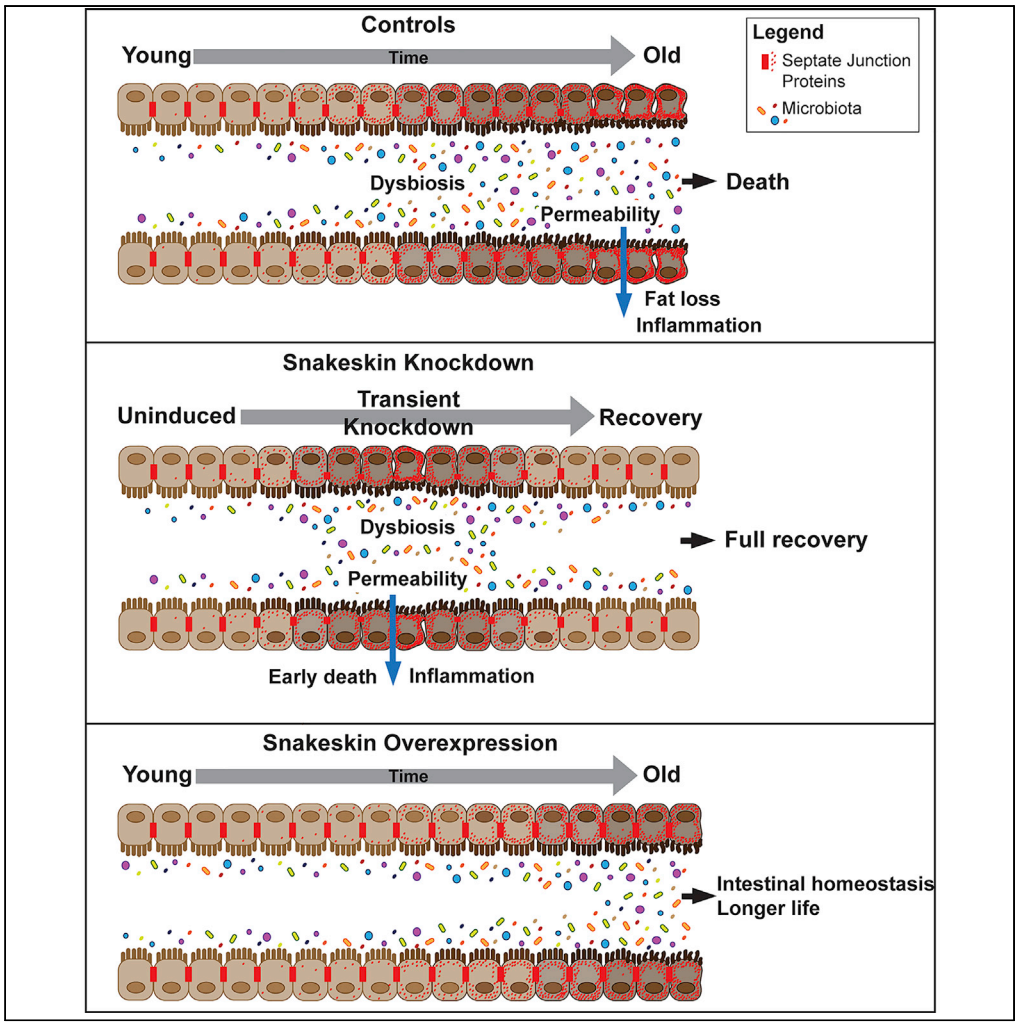

Anna M. Salazar, Martin Resnik-Docampo, Matthew Ulgherait, Rebecca I. Clark, Mimi Shirasu-Hiza, D. Leanne Jones, David W. Walker

davidwalker@ucla.edu

HIGHLIGHTS

Loss of Ssk leads to intestinal barrier dysfunction, dysbiosis, and early-onset death

Restoration of Ssk reverses each of these age-associated phenotypes

Up-regulation of Ssk prevents bacterial translocation upon pathogenic infection

Ssk up-regulation improves barrier integrity, limits dysbiosis, and extends lifespan

Salazar et al., iScience 9, 229–243
November 30, 2018
https://doi.org/10.1016/j.isci.2018.10.022

iScience

CellPress

Article

Intestinal Snakeskin Limits Microbial Dysbiosis during Aging and Promotes Longevity

Anna M. Salazar,[1] Martin Resnik-Docampo,[2] Matthew Ulgherait,[3] Rebecca I. Clark,[1,4] Mimi Shirasu-Hiza,[3] D. Leanne Jones,[2,5,6] and David W. Walker[1,6,7,*]

SUMMARY

Intestinal barrier dysfunction is an evolutionarily conserved hallmark of aging, which has been linked to microbial dysbiosis, altered expression of occluding junction proteins, and impending mortality. However, the interplay between intestinal junction proteins, age-onset dysbiosis, and lifespan determination remains unclear. Here, we show that altered expression of Snakeskin (Ssk), a septate junction-specific protein, can modulate intestinal homeostasis, microbial dynamics, immune activity, and lifespan in *Drosophila*. Loss of Ssk leads to rapid and reversible intestinal barrier dysfunction, altered gut morphology, dysbiosis, and dramatically reduced lifespan. Remarkably, restoration of Ssk expression in flies showing intestinal barrier dysfunction rescues each of these phenotypes previously linked to aging. Intestinal up-regulation of Ssk protects against microbial translocation following oral infection with pathogenic bacteria. Furthermore, intestinal up-regulation of Ssk improves intestinal barrier function during aging, limits dysbiosis, and extends lifespan. Our findings indicate that intestinal occluding junctions may represent prolongevity targets in mammals.

INTRODUCTION

The intestinal epithelium acts as a selectively permeable barrier that permits the absorption of nutrients, ions, and water, while maintaining an effective defense against intraluminal toxins, antigens, and enteric microorganisms. In recent years, studies in diverse organisms, including worms (Dambroise et al., 2016; Gelino et al., 2016), flies (Dambroise et al., 2016; Rera et al., 2011, 2012), fish (Dambroise et al., 2016), rodents (Thevaranjan et al., 2017), and primates (Mitchell et al., 2017; Tran and Greenwood-Van Meerveld, 2013), have shown that intestinal barrier dysfunction is a pathophysiological hallmark of aging (Hu and Jasper, 2017). Loss of intestinal barrier function, in aged flies, is linked to organismal health decline, including loss of motor activity, systemic metabolic defects, and impending mortality (Clark et al., 2015; Rera et al., 2012). In addition, numerous gastrointestinal and systemic diseases, including inflammatory bowel diseases (IBDs), diabetes, multiple sclerosis, heart disease, autism, and Parkinson disease, have been associated with barrier dysfunction of the intestine (Choi et al., 2017; Farhadi et al., 2003; Hu and Jasper, 2017). Together, these findings indicate that identification of molecular targets for therapeutic intervention to improve or restore intestinal barrier function holds promise toward the goal of prolonging both health span and lifespan.

Occluding junctions play critical roles in epithelial barrier function, restricting the free diffusion of solutes between cells, as well as in the regulation of paracellular transport. In vertebrates, the occluding junctions are called tight junctions and their functional roles are well characterized (Buckley and Turner, 2018). A functionally analogous structure, called the septate junction (SJ), exists in invertebrates. In arthropods, there exist two types of SJs with morphological differences: pleated SJs, which are found in ectodermally derived epithelial cells and glial cells, and the smooth SJs (sSJs), which are found in endodermally derived epithelia, such as the midgut (Tepass and Hartenstein, 1994). Patients with IBDs can display an increase in gut permeability, or "leaky gut," and changes in occluding junction expression (Odenwald and Turner, 2017). Although it is unclear what role occluding junction modulation plays in the initiation or perpetuation of IBDs, it has been proposed that the cellular machinery that maintains the intestinal barrier may represent a therapeutic target in both intestinal and systemic diseases (Odenwald and Turner, 2017).

Previous work in *Drosophila* has identified a number of age-related intestinal changes, including intestinal stem cell (ISC) deregulation (Biteau et al., 2008; Choi et al., 2008; Park et al., 2009), which are associated with

[1]Department of Integrative Biology and Physiology, University of California, Los Angeles, Los Angeles, CA 90095, USA

[2]Department of Molecular, Cell, and Developmental Biology, University of California, Los Angeles, Los Angeles, CA 90095, USA

[3]Department of Genetics and Development, Columbia University Medical Center, New York, NY 10032, USA

[4]Department of Biosciences, Durham University, Durham DH1 3LE, UK

[5]Broad Stem Cell Research Center, University of California, Los Angeles, Los Angeles, CA 90095, USA

[6]Molecular Biology Institute, University of California, Los Angeles, Los Angeles, CA 90095, USA

[7]Lead Contact

*Correspondence: davidwalker@ucla.edu

https://doi.org/10.1016/j.isci.2018.10.022

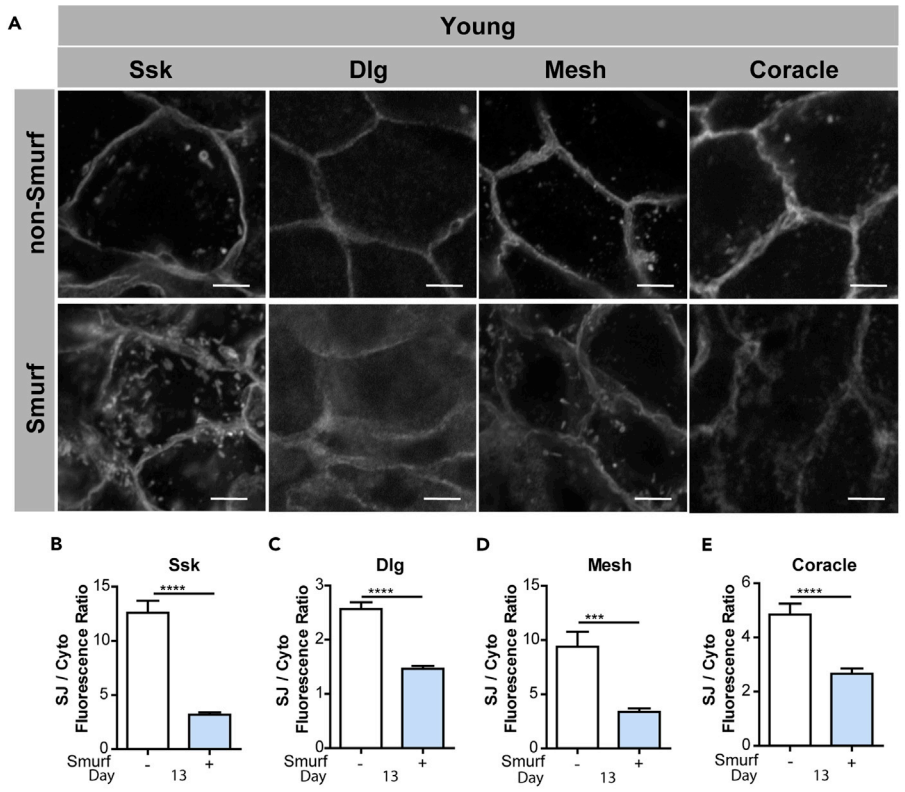
A
Young
Ssk
Dlg
Mesh
Coracle
non-Smurf
Smurf
B
Ssk
C
Dlg
D
Mesh
E
Coracle
SJ / Cyto Fluorescence Ratio
****
***
Smurf
Day
13
F
Midlife
G
H
I
J
30
*

Figure 1. Alterations in SJs in Posterior Midguts of Smurf and Non-Smurf Flies

(A–E) SJ protein localization in ECs in Smurf or Non-Smurf midguts in 13-day-old w^{1118} female flies. Representative images (A) and SJ/cytoplasm fluorescence ratios (B–E) for Ssk, Dlg, Mesh, and Coracle. SJ protein mislocalization is observed in Smurf ECs, represented by an increase in cytoplasmic localization. n ≥ 14 midguts per condition; n = 10 ECs were observed per midgut; scale bar, 5 μm.

(F–J) SJ protein localization in ECs in Smurf or non-Smurf midguts in 30-day-old w^{1118} female flies. Representative images (F) and SJ/cytoplasm fluorescence ratios (G–J) for Ssk, Dlg, Mesh, and Coracle. SJ protein mislocalization is observed in both Smurf and non-Smurf ECs, represented by an increase in cytoplasmic localization. n ≥ 14 midguts per condition; n = 10 ECs were observed per midgut; scale bar, 5 μm.

Samples were dissected and stained in parallel under the same conditions; pictures taken at same laser intensity. Data analyzed utilizing a two-tailed unpaired Student's t test, and the error bars are the SEM range of those averages. *$p < 0.05$; ***$p < 0.001$; ****$p < 0.0001$ represent a statistically significant difference. See also Figure S1.

a decline in intestinal function (Jasper, 2015). Age-related alterations in intestinal epithelial junction expression and localization have also been observed in both flies (Clark et al., 2015; Resnik-Docampo et al., 2017) and mammals (Meier and Sturm, 2009; Ren et al., 2014; Tran and Greenwood-Van Meerveld, 2013), yet the causal relationships between changes in occluding junction function, intestinal homeostasis, and organismal aging are only beginning to be understood. Recent work in *Drosophila* has shown that acute depletion of the tricellular junction (TCJ) protein, Gliotactin (Gli), in young flies leads to an increase in ISC proliferation and early-onset intestinal barrier dysfunction (Resnik-Docampo et al., 2017), indicating that altered TCJ function is sufficient to induce changes in ISC behavior previously observed in aged animals. Furthermore, age-related alterations in the composition and load of the intestinal microbiota have been shown to influence intestinal function and lifespan (Clark et al., 2015; Clark and Walker, 2018; Thevaranjan et al., 2017). Indeed, age-onset microbial dysbiosis is tightly linked to intestinal barrier dysfunction in both flies and mice (Clark et al., 2015; Thevaranjan et al., 2017). Critically, however, the question of whether manipulating intestinal occluding junction expression can delay age-onset dysbiosis and/or positively affect lifespan has not been addressed in any organism.

In this study, we show that Snakeskin (Ssk), an sSJ-specific protein (Furuse and Izumi, 2017; Yanagihashi et al., 2012), plays an important role in controlling the density and composition of the gut microbiota and that up-regulation of Ssk during aging can prolong *Drosophila* lifespan. More specifically, loss of intestinal Ssk in adults leads to rapid-onset intestinal barrier dysfunction, changes in gut morphology, altered expression of antimicrobial peptides (AMPs), and microbial dysbiosis. Critically, we show that these phenotypes, including intestinal barrier dysfunction and dysbiosis, can be reversed upon restored Ssk expression. Consistent with a critical role for intestinal junction proteins in organismal viability, loss of intestinal Ssk in adult animals leads to the rapid depletion of metabolic stores and rapid death. Importantly, restoring Ssk expression in flies showing intestinal barrier dysfunction prevents early-onset mortality. Moreover, intestinal up-regulation of Ssk in normal flies protects against microbial translocation, limits age-onset dysbiosis, and prolongs lifespan. Our findings support the idea that occluding junction modulation could prove an effective therapeutic approach to prolong both intestinal and organismal health during aging in other species, including mammals.

RESULTS

Alterations in Septate Junction Proteins Occur before the Smurf Phenotype

Loss of intestinal barrier function can be detected in living flies, via the Smurf assay, due to the leakage of a non-absorbable blue dye outside of the gut post-feeding (Rera et al., 2011, 2012). Previous work showed that flies exhibiting age-onset intestinal barrier dysfunction, or "Smurfs," display decreased expression of SJ and adherens junction (AJ) genes and proteins, relative to age-matched controls (Clark et al., 2015). Here, we utilized confocal immunofluorescence microscopy and quantitative PCR (qPCR) to further investigate the temporal dynamics between age-onset intestinal barrier dysfunction and alterations in junction protein localization or transcript expression. In young flies, aged 13 days, significant changes in the SJ proteins Discs large (Dlg), Coracle (Cora), Ssk, and Mesh were observed in the midgut of Smurf flies, and these SJ proteins appeared to accumulate in the cytoplasm (Figures 1A–1E). More specifically, in guts from Smurf flies, we observed an increase in junction proteins localized in the cytoplasm, relative to the plasma membrane, than in the non-Smurf flies, revealing that, in young flies, mislocalization of junction proteins is correlated with barrier dysfunction. In midlife, at age 30 days, we observed a mislocalization of SJ proteins occurring in both the non-Smurf and Smurf flies when compared with young non-Smurf flies (Figures 1F–1J). These data reveal that alterations in SJ proteins occur before the onset of the Smurf phenotype. Older flies,

aged 45 days, also showed no significant difference between Smurf and non-Smurf flies and exhibited severe mislocalization of SJ proteins (data not shown). Consistent with previous work (Resnik-Docampo et al., 2017), we failed to observe a decrease in transcript levels of SJ and AJ genes, in non-Smurfs during aging, indicating that downregulation of junction transcripts is not a primary mechanism underlying age-onset barrier dysfunction (Figures S1A–S1I). However, upon loss of intestinal barrier function, there is a decrease in mRNAs of genes encoding junction proteins (Clark et al., 2015).

Adult-Onset Loss of Ssk Leads to Reversible Intestinal Barrier Dysfunction

Loss of Ssk results in defective SJ formation and is embryonically lethal in *Drosophila* (Yanagihashi et al., 2012). In addition, it has been shown that RNAi-mediated depletion of Ssk in developing larvae impairs intestinal barrier function (Yanagihashi et al., 2012). Here, we set out to determine whether Ssk regulates intestinal barrier function in the adult gut. To do so, we utilized an RU486-inducible GeneSwitch driver that is expressed in gut enteroblasts (EBs) and post-mitotic enterocytes (ECs), *5966GS* (Mathur et al., 2010), crossed to a *UAS-ssk RNAi* line (Yanagihashi et al., 2012). Initially, we confirmed an RU486-dependent reduction in *ssk* expression in the adult intestine (Figure S2A). Upon adult onset, where flies were fed RU486 starting at the age of 3 days, intestine-specific *ssk* knockdown led to a rapid and pronounced decrease in intestinal barrier integrity (Figure 2A). Indeed, upon 7 days of *ssk* knockdown, 100% of female flies displayed the Smurf phenotype. Furthermore, adult-onset knockdown of *ssk* conferred early-onset mortality (Figure 2B). This observation is consistent with previous results showing that the Smurf phenotype is a harbinger of death in aging flies (Rera et al., 2012). Early-onset mortality also occurs when knockdown of *ssk* is initiated in midlife (day 35 or day 45, Figure S2B). In addition, adult-onset loss of intestinal Ssk leads to intestinal barrier dysfunction and early death in male flies (Figures S2C and S2D).

To better understand the role of *ssk* expression in barrier integrity in the adult intestine, we examined whether restoring *ssk* expression could rescue intestinal barrier function in Smurf flies. To do so, we examined the impact of transient knockdown of Ssk in the adult intestine. Following 7 days of RU486-mediated Ssk knockdown, after which time 100% of the flies displayed the Smurf phenotype, flies were allowed to recover for 1 week on food lacking RU486. Remarkably, we observed that upon restoration of *ssk* mRNA levels (Figure S3J), the Smurf phenotype is fully reversed, with the formerly Smurf flies now becoming non-Smurf ones (Figure 2C). Restoring intestinal barrier function in Smurf flies also prevented early-onset mortality (Figure 2D). Using an independently generated *UAS-ssk RNAi* line (VDRC, 11906GD, labeled *UAS-ssk RNAi* (*III*)), we confirmed that adult-onset intestinal knockdown of *ssk* led to reversible intestinal barrier dysfunction and early-onset mortality (Figures S2E–S2G). Feeding RU486 to control flies did not alter the intestinal barrier function or lifespan (Figures S2H and S2I). Consistent with the Smurf phenotype, electron microscopy revealed distinct gaps in SJs between adjacent ECs in midguts following intestinal knockdown of *ssk* (Figure 2E). This is completely reversed upon restoration of *ssk* mRNA levels, with the SJ becoming tight and no longer containing gaps between adjacent cells (Figure 2E).

Age-onset intestinal barrier dysfunction is linked to systemic metabolic defects, including reduced metabolic stores and impaired insulin/insulin growth factor signaling (Rera et al., 2012). Hence, we set out to determine whether acute loss of intestinal Ssk recapitulates these systemic metabolic phenotypes, previously linked to aging. Short-term, intestine-specific RNAi of *ssk* reduced survival on an agar-only diet (Figure 2F). This sensitivity to starvation was linked to reduced triglyceride stores (Figures 2G and 2H). One of the hallmarks of aging is the metabolic syndrome, also known as the insulin resistance syndrome, a clinical condition comprising physiological and biochemical abnormalities predisposing individuals to a host of age-onset diseases, including type 2 diabetes and cardiovascular disease (Lusis et al., 2008). In flies, aging and age-onset intestinal barrier dysfunction have been linked to *Drosophila* FOXO (dFOXO) activation (Guo et al., 2014; Morris et al., 2012; Rera et al., 2012), which is normally induced when IIS is repressed (Teleman, 2009). To gain insight into the impact of Ssk knockdown on dFOXO activation, we assayed the expression levels of two dFOXO target genes—*Insulin-like receptor* (*InR*) and *Ecdysone-inducible gene L2* (*ImpL2*). Both *InR* and *ImpL2* mRNA levels were significantly elevated in the intestine, following 6 days of *ssk* knockdown, and occurred before detectable barrier dysfunction (Figures S2J and S2K). In addition, *InR* and *ImpL2* mRNA levels returned to normal 1 week after transient *ssk* knockdown (Figures S2L and S2M), indicating that restoring intestinal Ssk rescues dFOXO activation. Feeding RU486 to control flies did not alter FOXO activation (Figures S2N and S2O), neither was a midlife elevation in FOXO targets observed in non-Smurfs (Figures S2P and S2Q).

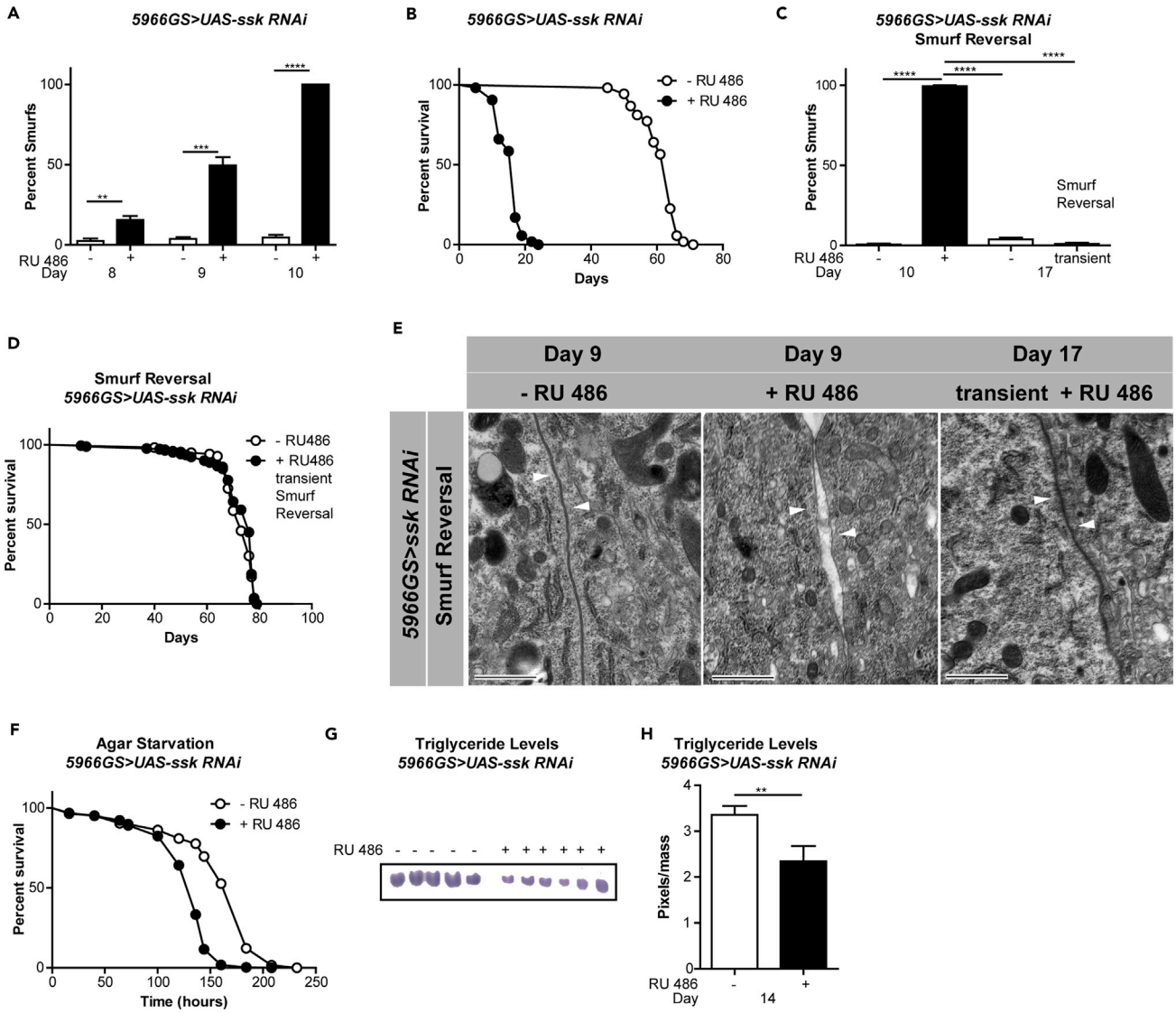

Figure 2. Loss of Intestinal Ssk Leads to Rapid and Reversible Intestinal Barrier Dysfunction and Early-Onset Mortality

(A) Intestinal integrity of *5966GS > UAS-ssk RNAi* females with or without RU486-mediated transgene induction from day 3 onward. Percentage Smurfs were assessed at 8, 9, and 10 days of age. One-way ANOVA/Bonferroni's multiple comparisons test; n > 179 flies/condition.

(B) Survival curves of *5966GS > UAS-ssk RNAi* females with or without RU486-mediated transgene induction from day 3 onward. p < .0001, log rank test; n > 107 flies/condition. Median lifespan 17 days and 64 days, respectively. Maximum lifespan 24 days and 71 days, respectively.

(C) Reversal of intestinal integrity of *5966GS > UAS-ssk RNAi* females with or without RU486-mediated transgene induction from day 3 until day 10, when all the induced flies become Smurfs, then moved to RU486− food for 7 days and assayed again for barrier integrity on day 17. n > 222/condition; p < 0.0001, one-way ANOVA/Bonferroni's multiple comparisons test.

(D) Survival curves of *5966GS > UAS-ssk RNAi* females with or without RU486-mediated transgene induction from day 3 to day 10, then without RU486-mediated transgene induction from day 10 onward. No statistical difference, log rank test; n > 182 flies/condition. Median lifespan 76 and 77 days, respectively.

(E) Electron micrographs of histological sections from dissected midguts of *5966GS > UAS-ssk RNAi* females with or without RU486-mediated transgene induction from day 3 to day 9 or transiently from day 3 until day 10, when all the induced flies become Smurfs, then moved to RU486− food for 7 days and imaged at day 17. Arrows point to SJ; scale bar, 800 nm.

(F) Survival curves without food of *5966GS > UAS-ssk RNAi* females at 9 days of age with or without RU486-mediated transgene induction from day 3 to day 9, then placed on agar until death. p < 0.0001; log rank test; n > 188 flies.

(G and H) Thin-layer chromatography image (G) and quantification (H) of whole-body lipid stores of *5966GS > UAS-ssk RNAi* females at 14 days of age with or without RU486-mediated transgene induction from day 3 to day 14. n = 5 and n = 6 biological replicates with five flies per replicate; p < 0.01; two-tailed unpaired Student's t test.

**p < 0.01; ***p < 0.001; ****p < 0.0001 represent a statistically significant difference. Error bars on bar graphs depict mean ± SEM. See also Figure S2.

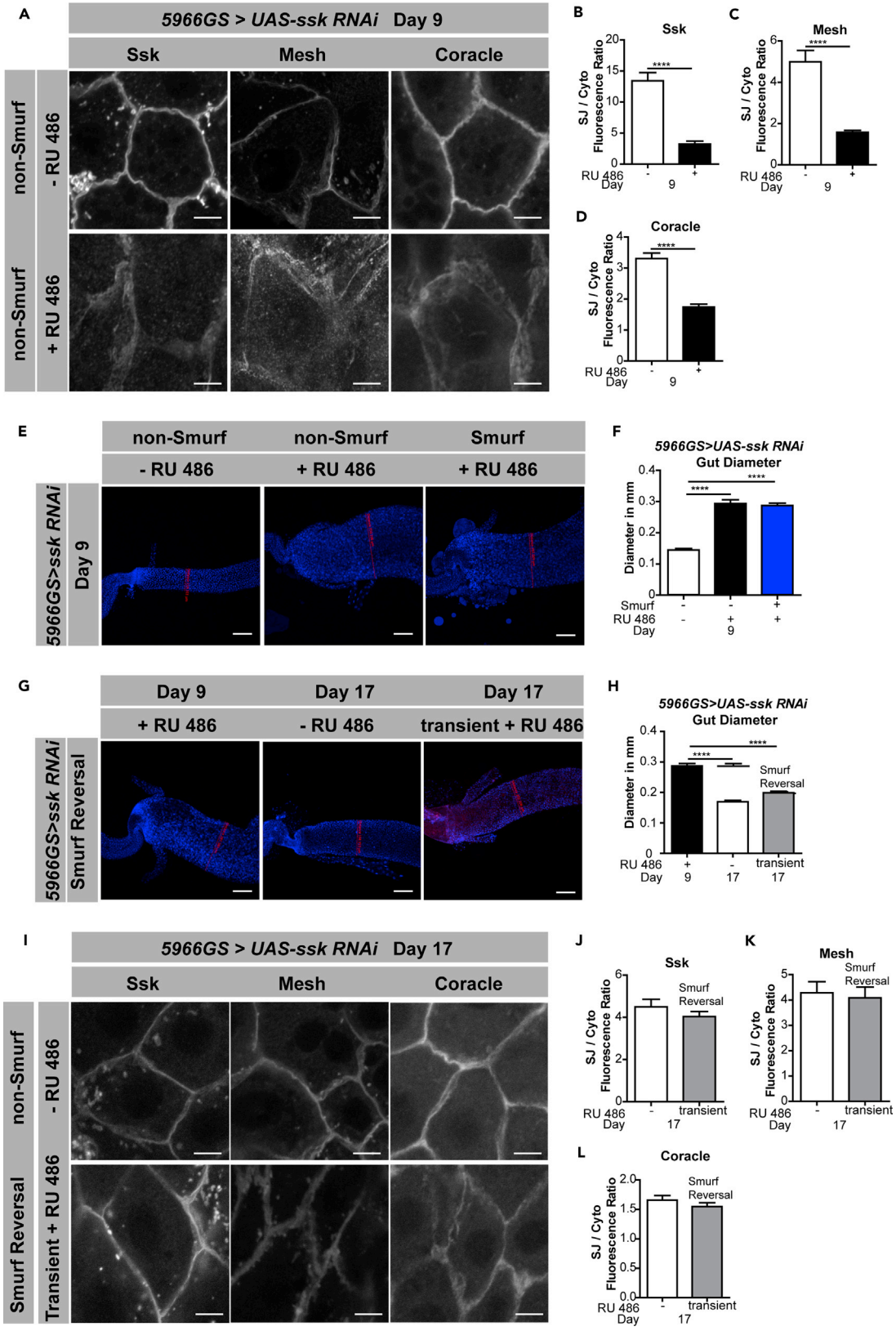
A
5966GS > UAS-ssk RNAi Day 9
Ssk
Mesh
Coracle
non-Smurf
- RU 486
non-Smurf
+ RU 486
B
Ssk
SJ / Cyto Fluorescence Ratio
RU 486
Day
C
Mesh
SJ / Cyto Fluorescence Ratio
RU 486
Day
D
Coracle
SJ / Cyto Fluorescence Ratio
RU 486
Day
E
non-Smurf
non-Smurf
Smurf
- RU 486
+ RU 486
+ RU 486
5966GS>ssk RNAi
Day 9
F
5966GS>UAS-ssk RNAi
Gut Diameter
Diameter in mm
Smurf
RU 486
Day
G
Day 9
Day 17
Day 17
+ RU 486
- RU 486
transient + RU 486
5966GS>ssk RNAi
Smurf Reversal
H
5966GS>UAS-ssk RNAi
Gut Diameter
Diameter in mm
Smurf Reversal
RU 486
Day
transient
I
5966GS > UAS-ssk RNAi Day 17
Ssk
Mesh
Coracle
non-Smurf
- RU 486
Smurf Reversal
Transient + RU 486
J
Ssk
Smurf Reversal
SJ / Cyto Fluorescence Ratio
RU 486
Day
transient
K
Mesh
Smurf Reversal
SJ / Cyto Fluorescence Ratio
RU 486
Day
transient
L
Coracle
Smurf Reversal
SJ / Cyto Fluorescence Ratio
RU 486
Day
transient

Figure 3. Loss of Intestinal Ssk Leads to Altered Gut Morphology and SJs

(A–D) SJ protein localization in ECs in 9-day-old *5966GS > UAS-ssk RNAi* female flies with RU486-mediated transgene induction from day 3 to day 9. Representative images (A) and SJ/cytoplasm fluorescence ratios for (B) Ssk, (C) Mesh, and (D) Coracle. SJ protein mislocalization is observed in the presence of RU486 ECs, represented by an increase in cytoplasmic localization. Two-tailed unpaired Student's t test. n > 14 midguts per condition; n = 10 ECs were observed per midgut; scale bar, 5 μm.

(E and F) Representative images (E) and quantification (F) of posterior midgut diameters from dissected intestines of *5966GS > UAS-ssk RNAi* female flies on day 9 with or without RU486-mediated transgene induction from day 3 to day 9. The red line shows the location measured. A significant increase in the midgut diameter is observed in Ssk knockdown flies in both Smurfs and non-Smurfs. n > 14 midguts per condition; scale bar, 50 μm.

(G and H) Representative images (G) and quantification (H) of posterior midgut diameters from dissected intestines of *5966GS > UAS-ssk RNAi* female flies on day 9 with RU486-mediated transgene induction from day 3 to day 9, or on day 17, with and without RU486-mediated transgene induction from day 3 to day 10 when all induced flies become Smurfs, then removed from RU486-mediated induction for 7 more days until day 17, where flies were assayed with blue dye, to now be non-Smurfs. The red line shows the location measured. Transiently induced midgut diameter has returned to control levels. n > 14 midguts per condition; scale bar, 50 μm.

(I–L) SJ protein localization in ECs in midguts of 17-day-old *5966GS > UAS-ssk RNAi* female flies with and without RU486-mediated transgene induction from day 3 to day 10 when all induced flies become Smurfs, then removed from RU486-mediated induction for 7 more days until day 17, where flies were assayed with blue dye, to now be non-Smurfs. Representative images (I) and SJ/cytoplasm fluorescence ratios for (J) Ssk, (K) Mesh and (L) Coracle. There was no significant difference in SJ protein localization, two-tailed unpaired t test. n > 14 midguts per condition; n = 10 ECs were observed per midgut; scale bar, 5 μm.

Samples were dissected and stained in parallel under same conditions, pictures taken at same laser intensity. Data analyzed with one-way ANOVA/Tukey's multiple comparisons test, unless otherwise stated, and the error bars are the SEM range of those averages. ****$p < 0.0001$ represent a statistically significant difference. See also Figure S3.

Ssk Knockdown Results in Mislocalization of Septate Junction Proteins and Altered Gut Morphology

Ssk forms a protein complex with Mesh and Tetraspanin 2A (Tsp2A), and each of these three components are necessary for SJ formation during development (Furuse and Izumi, 2017; Izumi et al., 2012). We set out to investigate the role of Ssk in the maintenance of the SJ in the adult midgut. Immunofluorescent images of SJ components revealed mislocalization of junction proteins following 6 days of Ssk knockdown (Figures 3A–3D and S3A). In addition to Ssk mislocalization, there was a mislocalization of Mesh and Cora, reinforcing the idea that Ssk is required for proper localization of other SJ components or maintenance of the SJ in the adult fly, similar to its role in larvae (Furuse and Izumi, 2017; Izumi et al., 2012). In addition to changes in protein localization, there was also a reduction in the transcripts of both SJ and AJ components upon Ssk knockdown (Figure S3B). These changes in gene expression occurred before the Smurf phenotype (Figures S3C–S3H). Interestingly, after 11 days of Ssk knockdown, when the flies are close to death, we observed an increase in junction gene mRNA levels (Figure S3I), consistent with findings in flies with acute loss of the TCJ protein Gli (Resnik-Docampo et al., 2017). In addition to changes in junction protein localization and gene expression, there was also a striking effect on gut morphology. Specifically, the posterior midgut appeared shorter and wider, with a diameter almost twice that of control guts (Figures 3E and 3F).

Remarkably, these alterations in gut morphology, occluding junction localization, and mRNA levels, that occurred following *ssk* knockdown, were also completely reversible. After inducing transient *ssk* knockdown for 7 days, until all the flies became Smurfs, followed by recovery of the Smurf flies on food lacking RU486 for 7 days, the gut morphology returned to control diameters (Figures 3G and 3H), SJ protein localization appeared normal (Figures 3I–3L), and junction gene mRNA levels returned to control levels (Figure S3J). Feeding RU486 to control flies did not alter mRNA levels of junction components, protein localization, or gut morphology in control flies (Figures S3K–S3Q). These findings illustrate that reducing the expression of Ssk causes the mislocalization of other SJ components, changes in gut morphology, and alterations in junction gene mRNA levels and that restoring Ssk expression reverses these changes.

Loss of Ssk Leads to Intestinal Stem Cell Overproliferation

The *Drosophila* midgut epithelium is composed of ISCs that self-renew to maintain the ISC population and generate daughter cells termed EBs that differentiate to produce the secretory enteroendocrine cells and absorptive ECs (Micchelli and Perrimon, 2006; Ohlstein and Spradling, 2006). During aging, and in response to intestinal damage or pathogenic infection, an increase in ISC proliferation is observed, which is accompanied by a block in terminal differentiation, whereby differentiating cells exhibit both ISC/EB and EC markers (Biteau et al., 2008; Buchon et al., 2009; Choi et al., 2008; Jiang et al., 2009; Park et al., 2009). As previous work had indicated that depletion of SJ components from ECs was sufficient to trigger ISC proliferation in young flies, similar to what was observed during aging (Resnik-Docampo et al., 2017), we wanted to assess stem cell proliferation upon adult-onset depletion of Ssk from intestinal ECs.

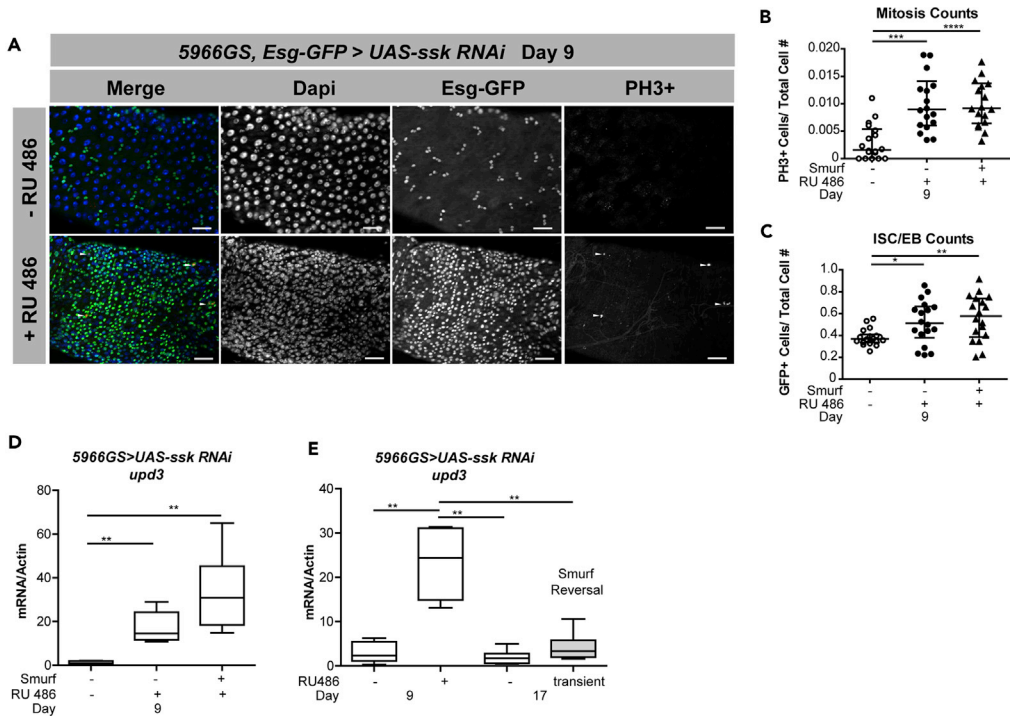

Figure 4. Loss of Intestinal Ssk Leads to Overproliferation of Intestinal Stem Cells

(A–C) Representative images (A) and quantification showing mitosis counts (B) and changes in ISC/EB number (C) of posterior midguts from dissected intestines of *5966GS, esg:GFP > UAS-ssk RNAi* female flies on day 9 with RU486-mediated transgene induction from day 3 to day 9. Ssk knockdown causes an increase in esg^{+}ISC/EBs (marked by esg:GFP, green) and ISC proliferation (marked by arrowheads PH3, red) compared with controls. Scale bar, 50 μm.

(B) $n = 18$ midguts/condition. Each data point is an average proportion calculated from four independent images per midgut, and the error bars represent the mean ± SEM of those averages; one-way ANOVA/Tukey's multiple comparisons test. ****$p < 0.0001$; ***$p < 0.001$. (C) $n = 17$ midguts/condition. Each data point is an average proportion calculated from four independent images per midgut, and the error bars represent the median with interquartile range of those averages. Kruskal-Wallis/Dunn multiple comparisons test. **$p < 0.01$; *$p < 0.05$.

(D) *upd3, unpaired3*, gene expression assayed by qPCR from dissected intestines in Smurf and non-Smurf *5966GS > UAS-ssk RNAi* female flies on day 9 with or without RU486-mediated transgene induction from day 3 to day 9. n = 6 replicates of five intestines.

(E) *upd3* gene expression assayed by qPCR from dissected intestines in *5966GS > UAS-ssk RNAi* female flies at 9 days of age with or without RU486-mediated transgene induction from day 3 until day 10, when all the induced flies become Smurfs, and then moved to RU486 food for 7 days and assayed on day 17. n = 6 replicates of five intestines.

Boxplots display the first and third quartile, with the horizontal bar at the median and whiskers showing the most extreme data point, which is no more than 1.5 times the interquartile range from the box. Wilcoxon test unless otherwise stated. See also Figure S4.

A pronounced increase in ISC proliferation and a decrease in terminal differentiation of progenitor cells was observed before Smurf detection (Figures 4A–4C), implying that the perturbation of SJs in the midgut of 9-day-old flies is sufficient to stimulate an increase in stem cell proliferation.

The Janus kinase/signal transducer and activator of transcription (JAK/STAT) pathway has been reported to stimulate ISC proliferation in response to damage, infection, or stress (Jiang et al., 2009; Resende and Jones, 2012). Hence, we examined the mRNA levels of *unpaired 3* (*upd3*), one of the cytokines that activates the JAK/STAT pathway in flies. Adult-onset depletion of Ssk resulted in elevations in *upd3* mRNA levels before Smurf detection (Figure 4D). Feeding RU486 to control flies did not affect *upd3* expression (Figure S4A). Moreover, when RU486 is removed, thereby eliminating Ssk knockdown, and the flies are allowed to recover for a week, *upd3* levels return to normal (Figure 4E). Interestingly, we observed a significant increase in *upd3* mRNA levels in non-Smurf flies in midlife (day 30; Figure S4B), corresponding to the mislocalization and altered expression of SJ-related proteins (Figure 1F), which is similar to the SJ protein modulation observed in aged flies (Resnik-Docampo et al., 2017). This suggests a correlation between

junctional protein mislocalization, activation of the JAK/STAT pathway, and initiation of stem cell overproliferation before detectable intestinal barrier failure.

Loss of Intestinal Ssk Leads to Reversible Microbial Dysbiosis

In both *Drosophila* and mice, age-onset intestinal barrier dysfunction is linked to microbial dysbiosis (Clark et al., 2015; Thevaranjan et al., 2017). Control of the commensal microbiota and innate immune responses to pathogenic bacteria are achieved primarily by two pathways acting in *Drosophila* gut ECs: expression and activation of dual oxidase (Duox), which initiates an oxidative burst response to produce high levels of reactive oxygen species (Ha et al., 2005, 2009a, 2009b), and activation of the immune deficiency (IMD/Relish) pathway, which activates the nuclear factor-κB-like transcription factor Relish and induces the expression of AMPs (Leulier and Royet, 2009). Previous studies have reported a large increase in AMP expression in flies showing age-onset intestinal barrier dysfunction (Clark et al., 2015; Rera et al., 2012). Therefore, we wanted to examine the relationship between immunity gene expression and intestinal Ssk expression. Short-term intestinal Ssk knockdown, for 6 days, led to a decrease in AMP expression (Figures 5A–5D), as well as decreased expression of Duox (Figure 5E). This reduction in immunity gene mRNA levels occurred in non-Smurf as well as Smurf flies (Figure S5A), revealing that this occurs before detectable barrier dysfunction. Feeding RU486 to control flies did not affect immunity gene expression in control flies (Figures S5B and S5C). Knockdown of Ssk for 11 days led to the activation of an immune response, with flies now exhibiting elevated AMPs and Duox levels (Figures S5D and S5E), which is consistent with previous data in aged Smurf flies (Clark et al., 2015; Rera et al., 2012).

To determine whether altered immune gene expression was linked to changes in gut bacteria, we utilized qPCR with universal primers to the bacterial 16S rRNA gene to characterize alterations in microbiota dynamics in response to loss of intestinal Ssk. Short-term intestinal Ssk knockdown, for 7 days, led to a significant elevation in bacterial loads (Figure 5F), with these changes occurring before Smurf detection (Figures S5F and S5G). Next, we utilized primers to the 16S rRNA gene that are specific to the classes Bacilli, Gammaproteobacteria, and Alphaproteobacteria (Clark et al., 2015). Upon knockdown of intestinal Ssk, there was an increase in Alphaproteobacteria and Bacilli (Figures S5H), with these changes also occurring before Smurf detection (Figures S5I). There was no significant change in Gammaproteobacteria (Figure S5J). Elevations in microbial content and dysbiosis were also observed upon knockdown of Ssk in aged flies (75 days old), implying that even when there are higher levels of commensal bacteria in aged flies, perturbing SJs can still have a significant impact on microbiota dynamics (Figures S5K and S5L). Strikingly, restoring Ssk in the adult intestine by removing RU486 led to restoration of commensal homeostasis after 7 days (Figures 5F–5H and S5M), which was maintained throughout the lifespan of the fly (Figures S5N and S5O). Together, these data support the idea that loss of Ssk, alone, can cause dysbiosis, which is reversible upon resumption of Ssk expression. Restoring Ssk expression for 7 days, which promotes commensal homeostasis, was associated with increased expression of certain AMPs, including a significant increase in Diptericin (Figures S5P and S5Q).

Loss of commensal control during aging, including a large increase in microbial load, impairs intestinal function and drives mortality in aged flies showing intestinal barrier dysfunction (Clark et al., 2015). Hence, we set out to examine whether dysbiosis in Ssk knockdown flies contributes to intestinal barrier dysfunction and/or limits lifespan. When flies were maintained under axenic conditions (Figure S5R) or fed antibiotics, intestinal knockdown of Ssk conferred rapid intestinal barrier dysfunction and mortality at a similar rate as in conventionally raised flies (Figures 5I, 5J, and S5S). In addition, under axenic conditions, intestinal Ssk knockdown still led to an increase in dFOXO targets, mislocalization of SJ components (data not shown), altered gut morphology, and an increase of *upd3*, with no significant alterations in AMP or Duox transcripts (Figures S5T–S5Y). Together, these findings indicate that loss of intestinal Ssk does not affect intestinal barrier function or lifespan via altered microbial dynamics or an altered immune response. This suggests that altering SJ integrity, by knocking down one critical component, is sufficient to lead to hallmarks of the aged gut and a greatly diminished lifespan, even in the absence of bacteria.

Up-Regulation of Ssk Prevents Bacterial Translocation upon Pathogenic Infection

Serratia marcescens is an entomopathogenic bacterium that opportunistically infects a wide range of hosts, including humans. If ingested by *Drosophila*, *S. marcescens* can traverse the intestinal epithelium into the body cavity, leading to death within 6 days (Nehme et al., 2007). Here, we set out to determine whether

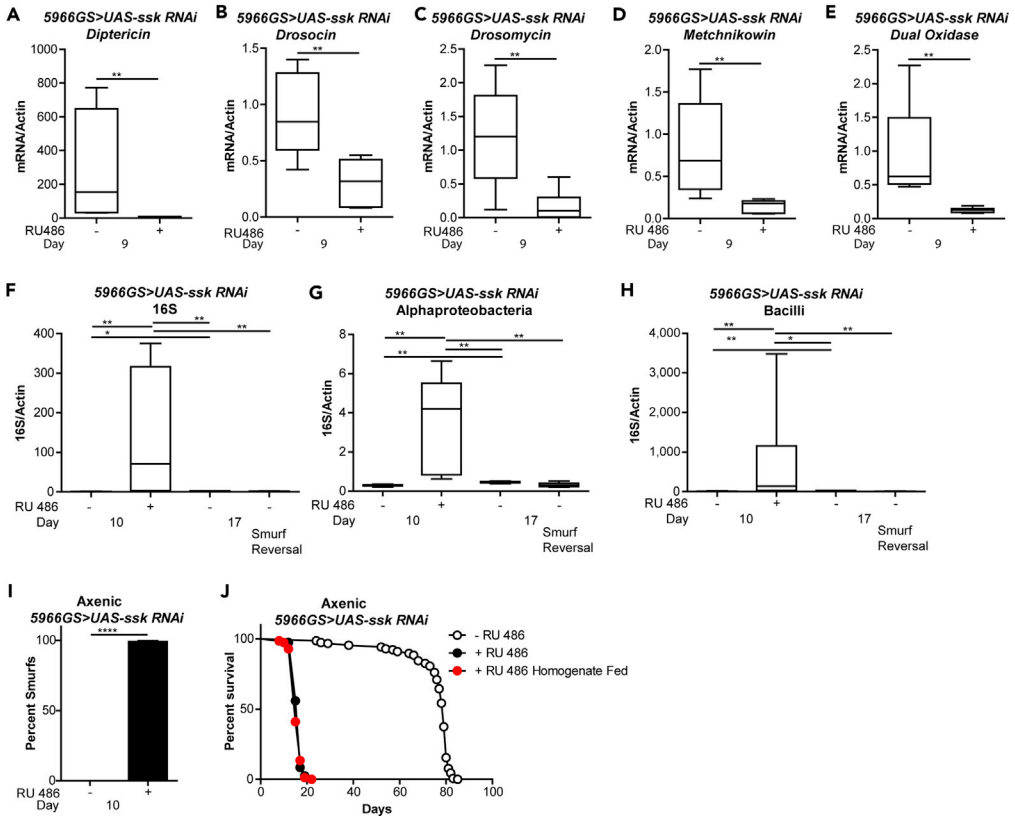

Figure 5. Loss of Intestinal Ssk Leads to Reversible Microbial Dysbiosis

(A–E) Immunity gene expression assayed by qPCR from dissected intestines of *5966GS > UAS-ssk RNAi* female flies on day 9 with or without RU486-mediated transgene induction from day 3 to day 9. *Diptericin* (A), *Drosocin* (B), *Drosomycin* (C), *Metchnikowin* (D), and *Dual Oxidase* (E). n = 6 replicates of five intestines per replicate.

(F) Reversal of bacterial levels assayed by qPCR of 16S with universal primers in surface-sterilized Smurf and non-Smurf *5966GS > UAS-ssk RNAi* female flies at 9 days of age with or without RU486-mediated transgene induction from day 3 to day 10, when all induced flies become Smurfs, then removed from RU486-mediated induction for 7 more days until day 17, where flies were assayed to now be non-Smurfs. n = 6 replicates of five whole flies per replicate.

(G and H) Reversal of bacterial levels assayed by taxon-specific qPCR of the *Alphaproteobacteria* or *Bacilli* 16S rRNA gene in *5966GS > UAS-ssk RNAi* female flies at 9 days of age with or without RU486-mediated transgene induction from day 3 to day 10, when all induced flies become Smurfs, then removed from RU486-mediated induction for 7 more days until day 17, where flies were assayed to now be non-Smurfs. n = 6 replicates of 5 whole flies per replicate.

(I) Intestinal integrity of axenic *5966GS > UAS-ssk RNAi* female flies at 10 days of age with or without RU486-mediated transgene induction from day 3 to day 10. $p < 0.0001$, two-tailed unpaired Student's t test; n > 155 flies/condition.

(J) Survival curves of *5966GS > UAS-ssk RNAi* females conventionally reared, axenically reared, and axenically treated and exposed to fly homogenate as embryos, with or without RU486-mediated transgene induction from day 3 onward. $p < .0001$, log rank test; n > 155 flies/condition. Boxplots display the first and third quartiles, with the horizontal bar at the median and whiskers showing the most extreme data point, which is no more than 1.5 times the interquartile range from the box. Error bars on bar graphs depict mean ± SEM.

*p < 0.05; **p < 0.01; ****p < 0.0001; Wilcoxon test unless otherwise stated. See also Figure S5.

manipulating Ssk expression can protect against *S. marcescens*-induced pathogenicity. To do so, we have used *S. marcescens* Db11 (Nehme et al., 2007). First, using a *UAS-ssk* transgene (Yanagihashi et al., 2012), we confirmed an RU486-dependent induction of *ssk* in the intestine (Figure S6A). Intestinal up-regulation of Ssk for 20 days resulted in a significant increase in survival following oral infection of Db11 (Figure 6A). Importantly, we observed no difference in bacterial loads in dissected guts following oral infection of Db11 (Figure 6B). However, intestinal up-regulation of Ssk led to a highly significant reduction in bacterial load in the hemolymph, which is the circulatory system of the fly (Figure 6C). These findings indicate that the up-regulation of Ssk can improve intestinal barrier integrity under these conditions to limit bacterial translocation. Feeding RU486 to control flies did not alter the lifespan or bacterial levels in the gut or hemolymph following oral infection of Db11 (Figures S6B–S6D).

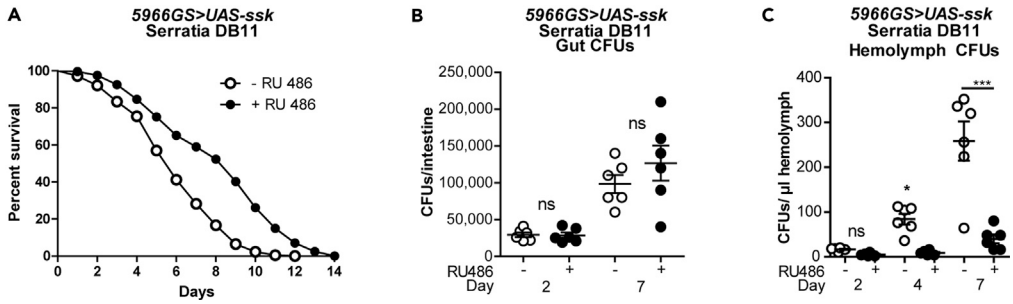

Figure 6. Intestinal Ssk Reduces Bacterial Translocation upon Oral Infection with Pathogenic Bacteria

(A) Survival curves of *5966GS* > *UAS-ssk* females with or without RU486-mediated transgene induction from day 3 until day 20; then Db11 bacteria were fed to the flies and survival plotted. $p < .0001$, log rank test; $n > 216$ flies/condition.

(B) *S. marcescens* Db11 colony-forming units (CFUs) from dissected midguts of *5966GS* > *UAS-ssk* females with or without RU486-mediated transgene induction from day 3 until day 20. There is no significant difference; one-way ANOVA/Tukey's multiple comparisons test. Error bars depict mean ± SEM.

(C) *S. marcescens* Db11 CFUs from the hemolymph of *5966GS* > *UAS-ssk* females with or without RU486-mediated transgene induction from day 3 until day 20. There is significantly less bacteria in the hemolymph when Ssk is up-regulated. ***$p < .0001$; one-way ANOVA/Tukey's multiple comparisons test. Error bars depict mean ± SEM.

See also Figure S6.

Up-Regulation of Ssk Improves Barrier Integrity, Limits Dysbiosis during Aging, and Extends Lifespan

Next, we set out to determine whether Ssk could improve intestinal homeostasis during aging and/or promote longevity. We overexpressed Ssk in wild-type flies and conducted a series of physiological assays to examine the impact of Ssk on aging and lifespan determination. Remarkably, we observed a delay in the onset of intestinal barrier dysfunction during aging upon intestinal Ssk up-regulation (Figure 7A). Moreover, intestinal up-regulation of Ssk resulted in a modest extension of lifespan when compared with isogenic controls (Figure 7B). Interestingly, on a diet containing yeast extract, which is more nutritionally dense than whole yeast (Bass et al., 2007), intestinal up-regulation of Ssk resulted in a more pronounced extension of lifespan (Figure 7C). This may be because as the concentration of yeast is increased, the bacterial load in control flies is elevated with a concomitant decrease in lifespan (Figures S7A and S7B). Up-regulating intestinal Ssk during aging also delayed the age-related increase in bacterial load and reduced the levels of both Alphaproteobacteria and Bacilli in aged animals (Figures 7D–7F and S7C). Importantly, the lifespan extension mediated by intestinal Ssk is eliminated when flies are either treated with antibiotics or raised under axenic conditions (Figures 7G and S7D). Together, our findings are consistent with a model in which up-regulating intestinal Ssk prolongs lifespan via improved commensal homeostasis.

DISCUSSION

Aging is characterized by progressive health decline leading to mortality, yet the underlying pathophysiology remains elusive. There is an emerging understanding that maintaining intestinal barrier function during aging is critical to organismal health and longevity (Cesar Machado and da Silva, 2016; Choi et al., 2017; Clark et al., 2015; Clark and Walker, 2018; Hu and Jasper, 2017; Rera et al., 2013; Rera et al., 2012; Thevaranjan et al., 2017). At the same time, an age-related remodeling of epithelial junctions has been implicated in loss of barrier function in aged animals (Clark et al., 2015; Meier and Sturm, 2009; Ren et al., 2014; Resnik-Docampo et al., 2017; Tran and Greenwood-Van Meerveld, 2013). These findings suggest that strategies to maintain epithelial junctions during aging may prove effective toward the goal of prolonging healthy lifespan. In this study, we have used the fruit fly, *Drosophila*, as a model to study the impact of altered expression of the SJ-specific protein Ssk on intestinal barrier function, commensal homeostasis, and lifespan. We show that Ssk is required to maintain barrier function and commensal homeostasis in the adult intestine. Indeed, loss of intestinal Ssk leads to rapid-onset microbial dysbiosis, immune gene modulation, barrier dysfunction, and mortality, although mortality was not due to dysbiosis. Furthermore, restoring Ssk led to resumption of barrier integrity and reversed these phenotypes, previously linked to aging. Remarkably, up-regulating Ssk in the adult intestine protected against oral infection with pathogenic bacteria. Improved survival under these conditions is linked to a reduction in

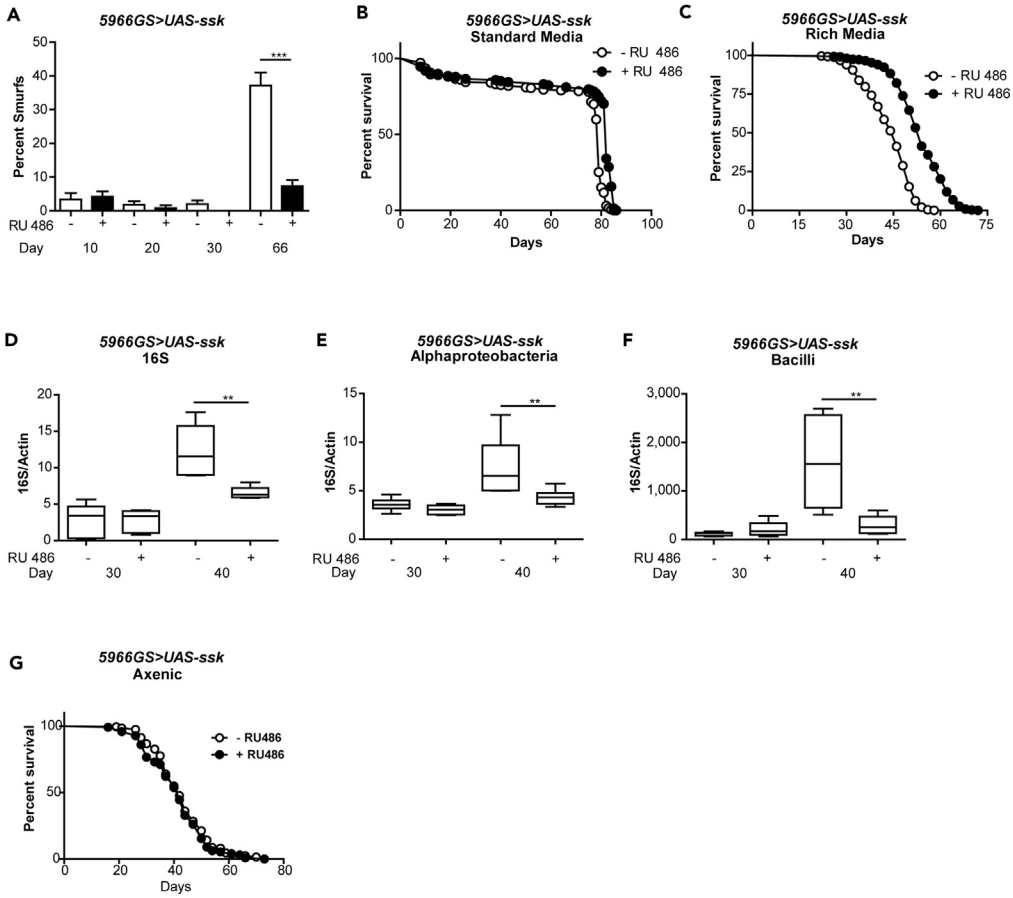

Figure 7. Up-Regulation of Ssk Improves Intestinal Integrity during Aging and Prolongs Lifespan

(A) Intestinal integrity of *5966GS > UAS-ssk* females with or without RU486-mediated transgene induction from day 3 onward on standard media. Percentage Smurfs were assessed with blue dye at 10, 20, 30, and 66 days of age. ***p < .0001, one-way ANOVA/Bonferroni's multiple comparisons test; n > 174 flies/condition.

(B) Survival curves of *5966GS > UAS-ssk* females with or without RU486-mediated transgene induction from day 3 onward on standard media. p < .0001, log rank test; n > 159 flies/condition. Median lifespan 79 and 82 days, respectively.

(C) Survival curves of *5966GS > UAS-ssk* females with or without RU486-mediated transgene induction from day 3 onward on rich media. p < .0001, log rank test; n > 288 flies/condition. Median lifespan 48 days and 54 days, respectively.

(D) Bacterial levels assayed by qPCR of 16S with universal primers in *5966GS > UAS-ssk* female flies at 30 and 40 days of age with or without RU486-mediated transgene induction from day 3 onward on rich media, n = 6 replicates of 5 flies.

(E and F) Bacterial levels assayed by taxon-specific qPCR of the *Alphaproteobacteria* or *Bacilli* 16S rRNA gene in *5966GS > UAS-ssk* female flies at 30 and 40 days of age with or without RU486-mediated transgene induction from day 3 onward on rich media, n = 6 replicates of 5 flies.

(G) Survival curves of axenic *5966GS > UAS-ssk* females with or without RU486-mediated transgene induction from day 3 onward on rich media. There was no significant difference, log rank test; n > 197 flies/condition. Median lifespan 42 days.

Boxplots display the first and third quartile, with the horizontal bar at the median and whiskers showing the most extreme data point, which is no more than 1.5 times the interquartile range from the box. Error bars on bar graphs depict mean ± SEM. **p < 0.01; ***p < 0.001; Wilcoxon test unless otherwise stated. See also Figure S7.

bacterial translocation, consistent with improved intestinal barrier function. Finally, intestinal overexpression of Ssk during aging delayed the onset of dysbiosis and intestinal barrier dysfunction and prolonged lifespan. The prolongevity effects of Ssk were eliminated when flies were maintained axenically, consistent with a key role for Ssk-mediated alterations in microbiota dynamics for its effects on longevity.

Previous work indicated that dysbiosis precedes and predicts intestinal barrier dysfunction in aged flies (Clark et al., 2015). Here, we show that there is a mislocalization of SJs during midlife, before the detection of intestinal barrier failure. Hence, it is possible that alterations in SJs occur either before or concurrent with

changes in microbial dynamics. It has previously been reported that age-related changes in SJ levels and localization were particularly noticeable at TCJs (Resnik-Docampo et al., 2017). Depletion of the *Drosophila* TCJ protein Gli led to ISC overproliferation and disruption of the intestinal barrier. Interestingly, however, acute loss of Gli does not lead to dysbiosis (Resnik-Docampo et al., 2017, 2018). This may be because TCJs contribute to only a small percentage of the barrier in the fly intestine, when compared with the bicellular junctions.

Ssk forms a complex with Mesh, another sSJ-specific protein, and these proteins are mutually interdependent for their localization (Furuse and Izumi, 2017; Izumi et al., 2012). Interestingly, it was recently reported that Mesh regulates *Duox* expression to modulate the load and composition of the gut microbiota (Xiao et al., 2017). Consistent with this model, we observe a significant inhibition of *Duox* expression upon intestinal Ssk knockdown. At the same time, however, we observe reduced expression of several AMPs in Ssk knockdown flies. Furthermore, we observe elevated AMP and Duox expression after longer periods of Ssk knockdown, which is consistent with previously observed AMP elevations observed in Smurf flies and in aged non-Smurf flies (Clark et al., 2015). These data demonstrate that knocking down one SJ protein that disturbs intestinal junction integrity leads to an initial repression of AMPs that coincides with rapid elevations in microbial load, followed by an increase in immune activation, before death. These data provide a possible mechanism for the initial increase in microbial content observed before detectable barrier permeability, yet recapitulate the later elevation in immune gene expression observed in aged flies. Further studies are required to determine the mechanistic relationships between SJs, immune homeostasis, and microbiota dynamics during aging.

In humans, compromised intestinal barrier function has been linked to a number of intestinal and systemic diseases (Choi et al., 2017). Although the existing clinical data have not established a causal role, the idea of targeting and restoring the intestinal epithelial barrier has been proposed as a potential therapeutic approach (Odenwald and Turner, 2017). A better understanding of the mechanisms underlying barrier regulation may aid this goal. At present, therapeutic approaches to treat intestinal barrier dysfunction have largely focused on reducing inflammation. Indeed, anti-tumor necrosis factor (TNF) therapy has been used to successfully treat intestinal barrier dysfunction in the context of Crohn disease (Noth et al., 2012; Suenaert et al., 2002). Consistent with this, TNF-deficient mice display improved intestinal barrier dysfunction during aging (Thevaranjan et al., 2017). Interestingly, anti-TNF therapy can reverse age-onset microbiota changes in mice (Thevaranjan et al., 2017). These data reveal that the composition of the microbiota can be altered by the inflammatory status of the host. Taken together, these studies support a model whereby an age-related increase in microbial translocation induces an inflammatory response, which contributes to dysbiosis. In this feedforward model, dysbiosis contributes to intestinal barrier dysfunction and increased microbial translocation (Thevaranjan et al., 2017). Previous work, in *Drosophila*, has shown that intestinal immune activation leads to intestinal barrier dysfunction and early-onset mortality (Clark et al., 2015). Our current study adds to this model by showing that occluding junction modulation can, by itself, induce dysbiosis and mortality. In fact, under axenic conditions, and in the absence of an inflammatory response, occluding junction modulation, alone, is sufficient to induce certain markers of aging and mortality. This is consistent with an important role for SJs in the feedforward model. Given our findings, it will be important to determine whether interventions that maintain the intestinal epithelial barrier in aging mammals can prolong intestinal and/or organismal health during aging.

Limitations of Study

Although *Drosophila melanogaster* is a well-studied and highly tractable model organism of proven utility in understanding mechanisms of aging, development, and disease, the relevance of molecular mechanisms uncovered in this work to human aging and disease remains to be demonstrated experimentally.

METHODS

All methods can be found in the accompanying Transparent Methods supplemental file.

SUPPLEMENTAL INFORMATION

Supplemental Information includes Transparent Methods and seven figures and can be found with this article online at https://doi.org/10.1016/j.isci.2018.10.022.

ACKNOWLEDGMENTS

We thank M. Furuse and the VDRC for fly stocks. In addition, stocks obtained from the Bloomington Drosophila Stock Center (NIH P40OD018537) were used in this study. We thank Chunni Zhu and the UCLA BRI Microscopic Techniques and Electron Microscopy Core Facility for help with electron microscopy. This work was supported by the NIH grants AG040288 (D.L.J. and D.W.W.), AG028092 and DK105442 (D.L.J.), AG049157 and AG037514 (D.W.W.), and GM105775 and AG045842 (M.S.-H.). M.U. is a Charles H. Revson Senior Fellow and supported by the NIH training grant 5T32DK007328. This research was conducted while D.W.W. was a Julie Martin Mid-Career Awardee in Aging Research supported by The Ellison Medical Foundation and AFAR.

AUTHOR CONTRIBUTIONS

A.M.S., M.R-D. and M.U. designed, performed, and analyzed experiments. R.I.C., M.S-H., D.L.J., and D.W.W designed and analyzed experiments. A.M.S. and D.W.W wrote the paper with input and comments from all authors.

DECLARATION OF INTERESTS

The authors declare no competing interests.

Received: May 21, 2018
Revised: September 24, 2018
Accepted: October 19, 2018
Published: November 30, 2018

REFERENCES

Bass, T.M., Grandison, R.C., Wong, R., Martinez, P., Partridge, L., and Piper, M.D. (2007). Optimization of dietary restriction protocols in *Drosophila*. J. Gerontol. A Biol. Sci. Med. Sci. *62*, 1071–1081.

Biteau, B., Hochmuth, C.E., and Jasper, H. (2008). JNK activity in somatic stem cells causes loss of tissue homeostasis in the aging *Drosophila* gut. Cell Stem Cell *3*, 442–455.

Buchon, N., Broderick, N.A., Chakrabarti, S., and Lemaitre, B. (2009). Invasive and indigenous microbiota impact intestinal stem cell activity through multiple pathways in *Drosophila*. Genes Dev. *23*, 2333–2344.

Buckley, A., and Turner, J.R. (2018). Cell biology of tight junction barrier regulation and mucosal disease. Cold Spring Harb. Perspect. Biol. *10*, 1–16.

Cesar Machado, M.C., and da Silva, F.P. (2016). Intestinal barrier dysfunction in human pathology and aging. Curr. Pharm. Des. *22*, 4645–4650.

Choi, N.-H., Kim, J.-G., Yang, D.-J., Kim, Y.-S., and Yoo, M.-A. (2008). Age-related changes in *Drosophila* midgut are associated with PVF2, a PDGF/VEGF-like growth factor. Aging Cell *7*, 318–334.

Choi, W., Yeruva, S., and Turner, J.R. (2017). Contributions of intestinal epithelial barriers to health and disease. Exp. Cell Res. *358*, 71–77.

Clark, R.I., Salazar, A., Yamada, R., Fitz-Gibbon, S., Morselli, M., Alcaraz, J., Rana, A., Rera, M., Pellegrini, M., Ja, W.W., et al. (2015). Distinct shifts in microbiota composition during *Drosophila* aging impair intestinal function and drive mortality. Cell Rep. *12*, 1656–1667.

Clark, R.I., and Walker, D.W. (2018). Role of gut microbiota in aging-related health decline: insights from invertebrate models. Cell. Mol. Life Sci. *75*, 93–101.

Dambroise, E., Monnier, L., Ruisheng, L., Aguilaniu, H., Joly, J.S., Tricoire, H., and Rera, M. (2016). Two phases of aging separated by the Smurf transition as a public path to death. Sci. Rep. *6*, 23523.

Farhadi, A., Banan, A., Fields, J., and Keshavarzian, A. (2003). Intestinal barrier: an interface between health and disease. J. Gastroenterol. Hepatol. *18*, 479–497.

Furuse, M., and Izumi, Y. (2017). Molecular dissection of smooth septate junctions: understanding their roles in arthropod physiology. Ann. N. Y Acad. Sci. *1397*, 17–24.

Gelino, S., Chang, J.T., Kumsta, C., She, X., Davis, A., Nguyen, C., Panowski, S., and Hansen, M. (2016). Intestinal autophagy improves healthspan and longevity in *C. elegans* during dietary restriction. PLoS Genet. *12*, e1006135.

Guo, L., Karpac, J., Tran, S.L., and Jasper, H. (2014). PGRP-SC2 promotes gut immune homeostasis to limit commensal dysbiosis and extend lifespan. Cell *156*, 109–122.

Ha, E.M., Lee, K.A., Park, S.H., Kim, S.H., Nam, H.J., Lee, H.Y., Kang, D., and Lee, W.J. (2009a). Regulation of DUOX by the galphaq-phospholipase Cbeta-Ca2+ pathway in *Drosophila* gut immunity. Dev. Cell *16*, 386–397.

Ha, E.M., Lee, K.A., Seo, Y.Y., Kim, S.H., Lim, J.H., Oh, B.H., Kim, J., and Lee, W.J. (2009b). Coordination of multiple dual oxidase-regulatory pathways in responses to commensal and infectious microbes in *Drosophila* gut. Nat. Immunol. *10*, 949–957.

Ha, E.M., Oh, C.T., Bae, Y.S., and Lee, W.J. (2005). A direct role for dual oxidase in *Drosophila* gut immunity. Science *310*, 847–850.

Hu, D.J., and Jasper, H. (2017). Epithelia: understanding the cell biology of intestinal barrier dysfunction. Curr. Biol. *27*, R185–R187.

Izumi, Y., Yanagihashi, Y., and Furuse, M. (2012). A novel protein complex, Mesh-Ssk, is required for septate junction formation in the *Drosophila* midgut. J. Cell Sci. *125*, 4923–4933.

Jasper, H. (2015). Exploring the physiology and pathology of aging in the intestine of *Drosophila melanogaster*. Invertebr. Reprod. Dev. *59*, 51–58.

Jiang, H., Patel, P.H., Kohlmaier, A., Grenley, M.O., McEwen, D.G., and Edgar, B.A. (2009). Cytokine/Jak/Stat signaling mediates regeneration and homeostasis in the *Drosophila* midgut. Cell *137*, 1343–1355.

Leulier, F., and Royet, J. (2009). Maintaining immune homeostasis in fly gut. Nat. Immunol. *10*, 936–938.

Lusis, A.J., Attie, A.D., and Reue, K. (2008). Metabolic syndrome: from epidemiology to systems biology. Nat. Rev. Genet. *9*, 819–830.

Mathur, D., Bost, A., Driver, I., and Ohlstein, B. (2010). A transient niche regulates the specification of *Drosophila* intestinal stem cells. Science *327*, 210–213.

Meier, J., and Sturm, A. (2009). The intestinal epithelial barrier: does it become impaired with age? Dig. Dis. *27*, 240–245.

Micchelli, C.A., and Perrimon, N. (2006). Evidence that stem cells reside in the adult *Drosophila* midgut epithelium. Nature *439*, 475–479.

Mitchell, E.L., Davis, A.T., Brass, K., Dendinger, M., Barner, R., Gharaibeh, R., Fodor, A.A., and Kavanagh, K. (2017). Reduced Intestinal motility, mucosal barrier function, and inflammation in aged monkeys. J. Nutr. Health Aging *21*, 354–361.

Morris, S.N., Coogan, C., Chamseddin, K., Fernandez-Kim, S.O., Kolli, S., Keller, J.N., and Bauer, J.H. (2012). Development of diet-induced insulin resistance in adult *Drosophila melanogaster*. Biochim. Biophys. Acta *1822*, 1230–1237.

Nehme, N.T., Liegeois, S., Kele, B., Giammarinaro, P., Pradel, E., Hoffmann, J.A., Ewbank, J.J., and Ferrandon, D. (2007). A model of bacterial intestinal infections in *Drosophila melanogaster*. PLoS Pathog. *3*, e173.

Noth, R., Stuber, E., Hasler, R., Nikolaus, S., Kuhbacher, T., Hampe, J., Bewig, B., Schreiber, S., and Arlt, A. (2012). Anti-TNF-alpha antibodies improve intestinal barrier function in Crohn's disease. J. Crohns Colitis *6*, 464–469.

Odenwald, M.A., and Turner, J.R. (2017). The intestinal epithelial barrier: a therapeutic target? Nat. Rev. Gastroenterol. Hepatol. *14*, 9–21.

Ohlstein, B., and Spradling, A. (2006). The adult *Drosophila* posterior midgut is maintained by pluripotent stem cells. Nature *439*, 470–474.

Park, J.-S., Kim, Y.-S., and Yoo, M.-A. (2009). The role of p38b MAPK in age-related modulation of intestinal stem cell proliferation and differentiation in *Drosophila*. Aging *1*, 637–651.

Ren, W.Y., Wu, K.F., Li, X., Luo, M., Liu, H.C., Zhang, S.C., and Hu, Y. (2014). Age-related changes in small intestinal mucosa epithelium architecture and epithelial tight junction in rat models. Aging Clin. Exp. Res. *26*, 183–191.

Rera, M., Azizi, M.J., and Walker, D.W. (2013). Organ-specific mediation of lifespan extension: more than a gut feeling? Ageing Res. Rev. *12*, 436–444.

Rera, M., Bahadorani, S., Cho, J., Koehler, C.L., Ulgherait, M., Hur, J.H., Ansari, W.S., Lo, T., Jr., Jones, D.L., and Walker, D.W. (2011). Modulation of longevity and tissue homeostasis by the *Drosophila* PGC-1 homolog. Cell Metab. *14*, 623–634.

Rera, M., Clark, R.I., and Walker, D.W. (2012). Intestinal barrier dysfunction links metabolic and inflammatory markers of aging to death in *Drosophila*. Proc. Natl. Acad. Sci. U S A *109*, 21528–21533.

Resende, L.P., and Jones, D.L. (2012). Local signaling within stem cell niches: insights from *Drosophila*. Curr. Opin. Cell Biol. *24*, 225–231.

Resnik-Docampo, M., Koehler, C.L., Clark, R.I., Schinaman, J.M., Sauer, V., Wong, D.M., Lewis, S., D'Alterio, C., Walker, D.W., and Jones, D.L. (2017). Tricellular junctions regulate intestinal stem cell behaviour to maintain homeostasis. Nat. Cell Biol. *19*, 52–59.

Resnik-Docampo, M., Sauer, V., Schinaman, J.M., Clark, R.I., Walker, D.W., and Jones, D.L. (2018). Keeping it tight: the relationship between bacterial dysbiosis, septate junctions, and the intestinal barrier in *Drosophila*. Fly (Austin) *12*, 1–7.

Suenaert, P., Bulteel, V., Lemmens, L., Noman, M., Geypens, B., Van Assche, G., Geboes, K., Ceuppens, J.L., and Rutgeerts, P. (2002). Anti-tumor necrosis factor treatment restores the gut barrier in Crohn's disease. Am. J. Gastroenterol. *97*, 2000–2004.

Teleman, A.A. (2009). Molecular mechanisms of metabolic regulation by insulin in *Drosophila*. Biochem. J. *425*, 13–26.

Tepass, U., and Hartenstein, V. (1994). The development of cellular junctions in the *Drosophila* embryo. Dev. Biol. *161*, 563–596.

Thevaranjan, N., Puchta, A., Schulz, C., Naidoo, A., Szamosi, J.C., Verschoor, C.P., Loukov, D., Schenck, L.P., Jury, J., Foley, K.P., et al. (2017). Age-associated microbial dysbiosis promotes intestinal permeability, systemic inflammation, and macrophage dysfunction. Cell Host Microbe *21*, 455–466.e4.

Tran, L., and Greenwood-Van Meerveld, B. (2013). Age-associated remodeling of the intestinal epithelial barrier. J. Gerontol. A Biol. Sci. Med. Sci. *68*, 1045–1056.

Xiao, X., Yang, L., Pang, X., Zhang, R., Zhu, Y., Wang, P., Gao, G., and Cheng, G. (2017). A Mesh-Duox pathway regulates homeostasis in the insect gut. Nat. Microbiol. *2*, 17020.

Yanagihashi, Y., Usui, T., Izumi, Y., Yonemura, S., Sumida, M., Tsukita, S., Uemura, T., and Furuse, M. (2012). Snakeskin, a membrane protein associated with smooth septate junctions, is required for intestinal barrier function in *Drosophila*. J. Cell Sci. *125*, 1980–1990.

ISCI, Volume *9*

Supplemental Information

Intestinal Snakeskin Limits Microbial Dysbiosis during Aging and Promotes Longevity

Anna M. Salazar, Martin Resnik-Docampo, Matthew Ulgherait, Rebecca I. Clark, Mimi Shirasu-Hiza, D. Leanne Jones, and David W. Walker

Supplemental Information

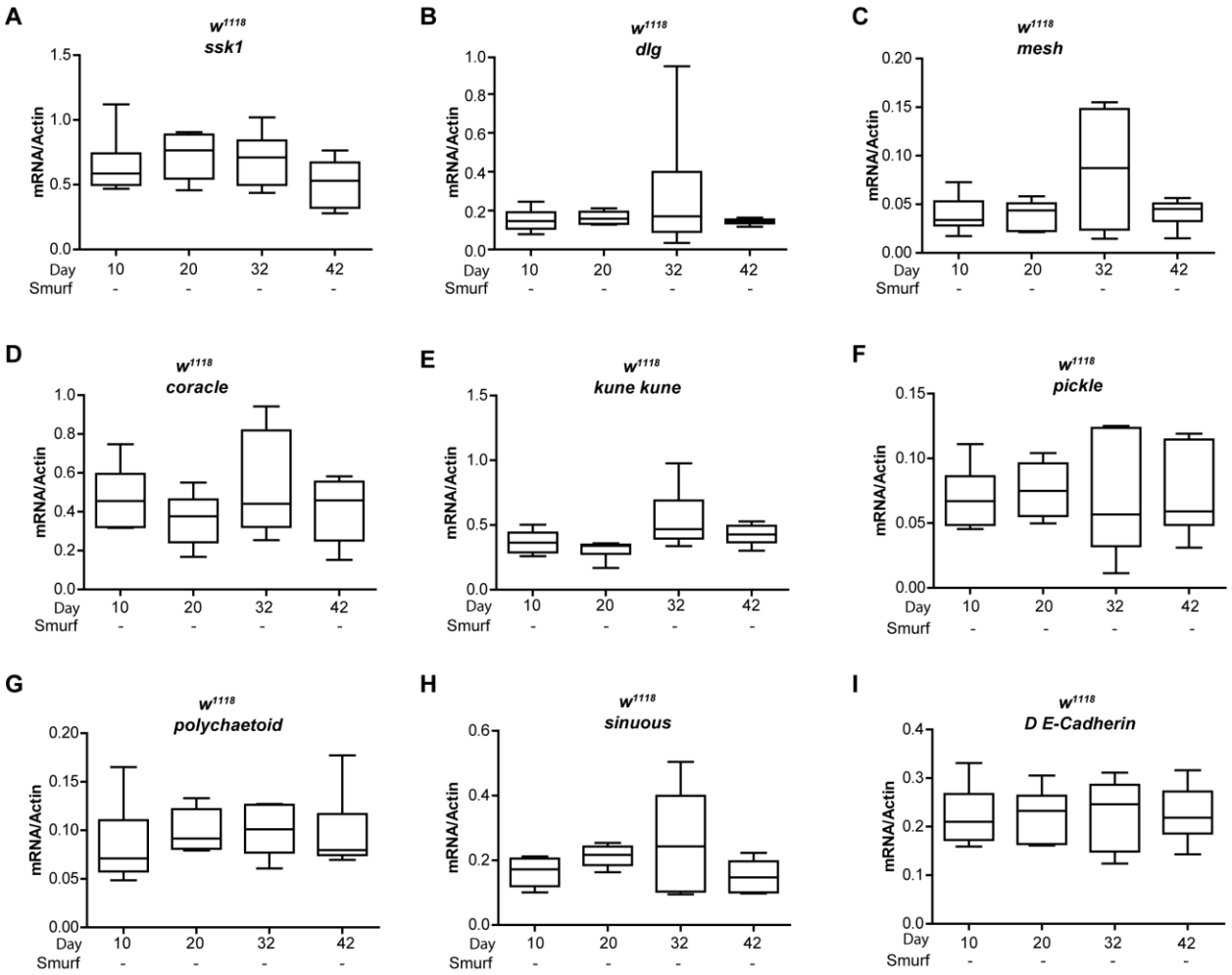

Figure S1. Alterations in SJs in posterior midguts of Smurf and non-Smurf flies. Related to Figure 1

(A-I) Junction protein gene expression assayed by qPCR from dissected intestines of w^{1118} non-Smurf (Smurf -) female flies at 10, 20, 32, and 42 days of age. n = 6 replicates of five intestines. *ssk, Snakeskin; dlg1, discs large 1; mesh; coracle; kune-kune; pickle; polychaetoid; sinuous; D E-Cadherin, Drosophila E-Cadherin.*

Boxplots display the first and third quartile, with the horizontal bar at the median and whiskers showing the most extreme data point, which is no more than 1.5 times the interquartile range from the box. No significant difference; Wilcoxon test.

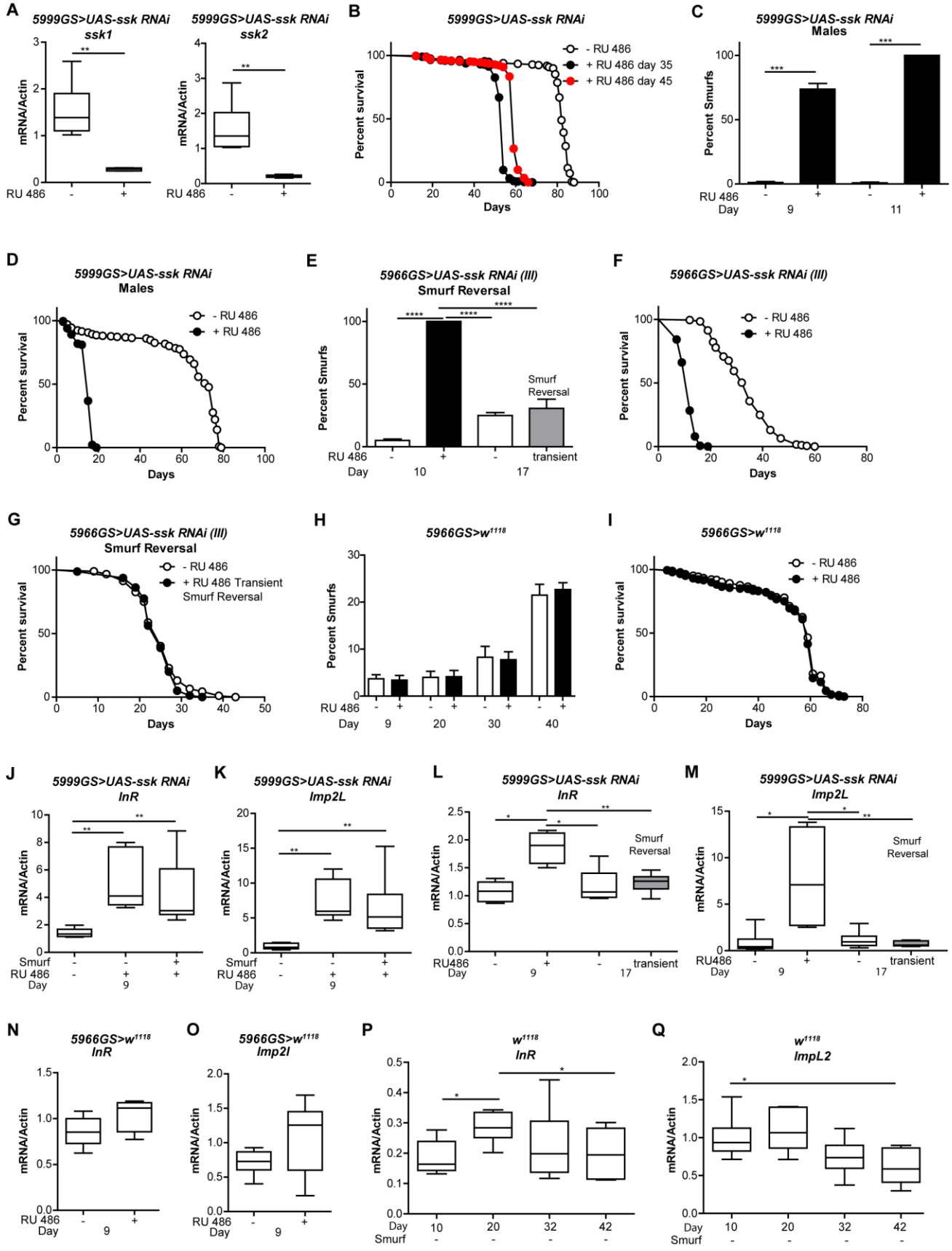
A
5999GS>UAS-ssk RNAi
ssk1
mRNA/Actin
RU 486
5999GS>UAS-ssk RNAi
ssk2
B
5999GS>UAS-ssk RNAi
- RU 486
+ RU 486 day 35
+ RU 486 day 45
Percent survival
Days
C
5999GS>UAS-ssk RNAi
Males
Percent Smurfs
Day
D
5999GS>UAS-ssk RNAi
Males
E
5966GS>UAS-ssk RNAi (III)
Smurf Reversal
Smurf Reversal
transient
F
5966GS>UAS-ssk RNAi (III)
G
5966GS>UAS-ssk RNAi (III)
Smurf Reversal
+ RU 486 Transient Smurf Reversal
H
5966GS>w1118
I
5966GS>w1118
J
5999GS>UAS-ssk RNAi
InR
Smurf
K
5999GS>UAS-ssk RNAi
Imp2L
L
5999GS>UAS-ssk RNAi
InR
M
5999GS>UAS-ssk RNAi
Imp2L
N
5966GS>w1118
InR
O
5966GS>w1118
Imp2l
P
w1118
InR
Q
w1118
ImpL2

Figure S2. Loss of intestinal Ssk leads to rapid and reversible intestinal barrier dysfunction and early-onset mortality. Related to Figure 2

(A) *ssk* gene expression assayed by qPCR utilizing two different sets of primers: *ssk1* and *ssk2,* from dissected intestines of *5966GS > UAS-ssk RNAi* female flies at 9 days of age with or without RU486-mediated transgene induction from day 3 to day 9. n = 6 replicates of five intestines.

(B) Survival curves of *5966GS>UAS-ssk RNAi* females with or without RU486-mediated transgene induction from day 35 or 45 onwards. $p < .0001$, log rank test; n > 196 flies/condition. Median lifespan 54, 59, and 82 days, respectively.

(C) Intestinal integrity of *5966GS>UAS-ssk RNAi* males with or without RU486-mediated transgene induction from day 3 onwards. Percentage Smurfs were assessed at 9 and 11 days of age. One-way ANOVA/Bonferroni's multiple comparisons test; n > 188 flies/condition.

(D) Survival curves of *5966GS>UAS-ssk RNAi* males with or without RU486-mediated transgene induction from day 3 onwards. $p < .0001$, log rank test; n > 231 flies/condition. Median lifespan 15 and 73 days, respectively.

(E) Reversal of intestinal integrity of *5966GS>UAS-ssk RNAi (III),* a different *ssk RNAi* line, females with or without RU486-mediated transgene induction from day 3 until day 10, when all of the induced flies become Smurfs, then moved to RU486- food for 7 days and assayed again for barrier integrity on day 17. One-way ANOVA/Bonferroni's multiple comparisons test; n > 177/condition.

(F) Survival curves of *5966GS>UAS-ssk RNAi (III)* females with or without RU486-mediated transgene induction from day 3 onwards. $p < .0001$, log rank test; n > 177 flies/condition. Median lifespan 12 and 35 days, respectively.

(G) Survival curves with reversal of early death of *5966GS>UAS-ssk RNAi (III)* females with or without RU486-mediated transgene induction from day 3 to day 10, then without RU486-mediated transgene induction from day 10 onwards. There is no significant difference, log rank test; n > 80 flies/condition. Median lifespan 25 days for each.

(H) Intestinal integrity of *5966GS>w^{1118}* females with or without RU486-mediated transgene induction from day 3 onwards. Percentage Smurfs were assessed at 9 and 11 days of age. There is no significant difference, one-way ANOVA/Bonferroni's multiple comparisons test; n > 267 flies/condition.

(I) Survival curves of *5966GS>w^{1118}* females with or without RU486-mediated transgene induction from day 3 onwards. There is no significant difference, log rank test; n > 267 flies/condition. Median lifespan 59 and 59 days, respectively.

(J and K) FOXO target gene expression assayed by qPCR from dissected intestines in Smurf and non-Smurf *5966GS>UAS-ssk RNAi* female flies on day 9 with or without RU486-mediated transgene induction from day 3 to day 9. *Insulin-like Receptor, InR*; Ecdysone-inducible gene L2, *ImpL2;* n = 6 replicates of five intestines.

(L and M) Reversal of FOXO target gene expression assayed by qPCR from dissected intestines in *5966GS>UAS-ssk RNAi* female flies at 9 days of age with or without RU486-mediated transgene induction from day 3 until day 10, when all of the induced flies become Smurfs, then moved to food lacking RU486 for 7 days and assayed on day 17. *Insulin-like Receptor, InR*; Ecdysone-inducible gene L2, *ImpL2*; n = 6 replicates of five intestines.

(N and O) FOXO target gene expression assayed by qPCR from dissected intestines in *5966GS>w^{1118}* female flies on day 9 with or without RU486-mediated transgene induction from day 3 to day 9. *Insulin-like Receptor, InR*; Ecdysone-inducible gene L2, *ImpL2*; n = 6 replicates of five intestines.

(P and Q) FOXO target gene expression assayed by qPCR from dissected intestines in *w^{1118}* non-Smurf (Smurf -) female flies at 10, 20, 32, and 42 days of age. *Insulin-like Receptor, InR*; Ecdysone-inducible gene L2, *ImpL2*; n = 6 replicates of five intestines.

Boxplots display the first and third quartile, with the horizontal bar at the median and whiskers showing the most extreme data point, which is no more than 1.5 times the interquartile range from the box. Error bars on bar graphs depict mean ± SEM. *$p < 0.05$; **$p < 0.01$; ***$p < 0.001$; ****$p < 0.0001$ represent a statistically significant difference. Wilcoxon test unless otherwise stated.

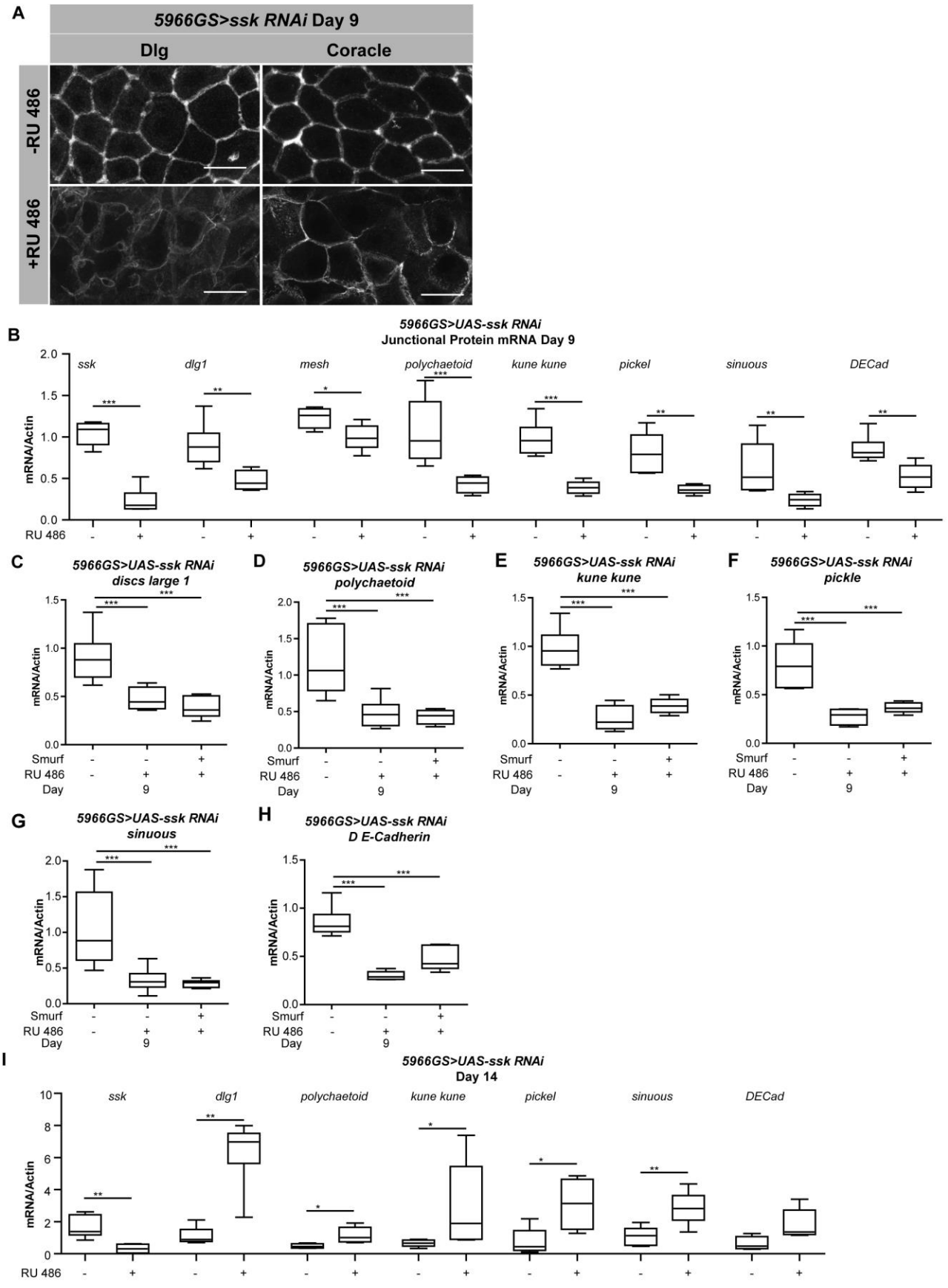
A
5966GS>ssk RNAi Day 9
Dlg
Coracle
-RU 486
+RU 486
B
5966GS>UAS-ssk RNAi
Junctional Protein mRNA Day 9
ssk
dlg1
mesh
polychaetoid
kune kune
pickel
sinuous
DECad
mRNA/Actin
RU 486
C
5966GS>UAS-ssk RNAi
discs large 1
D
5966GS>UAS-ssk RNAi
polychaetoid
E
5966GS>UAS-ssk RNAi
kune kune
F
5966GS>UAS-ssk RNAi
pickle
Smurf
RU 486
Day
G
5966GS>UAS-ssk RNAi
sinuous
H
5966GS>UAS-ssk RNAi
D E-Cadherin
I
5966GS>UAS-ssk RNAi
Day 14

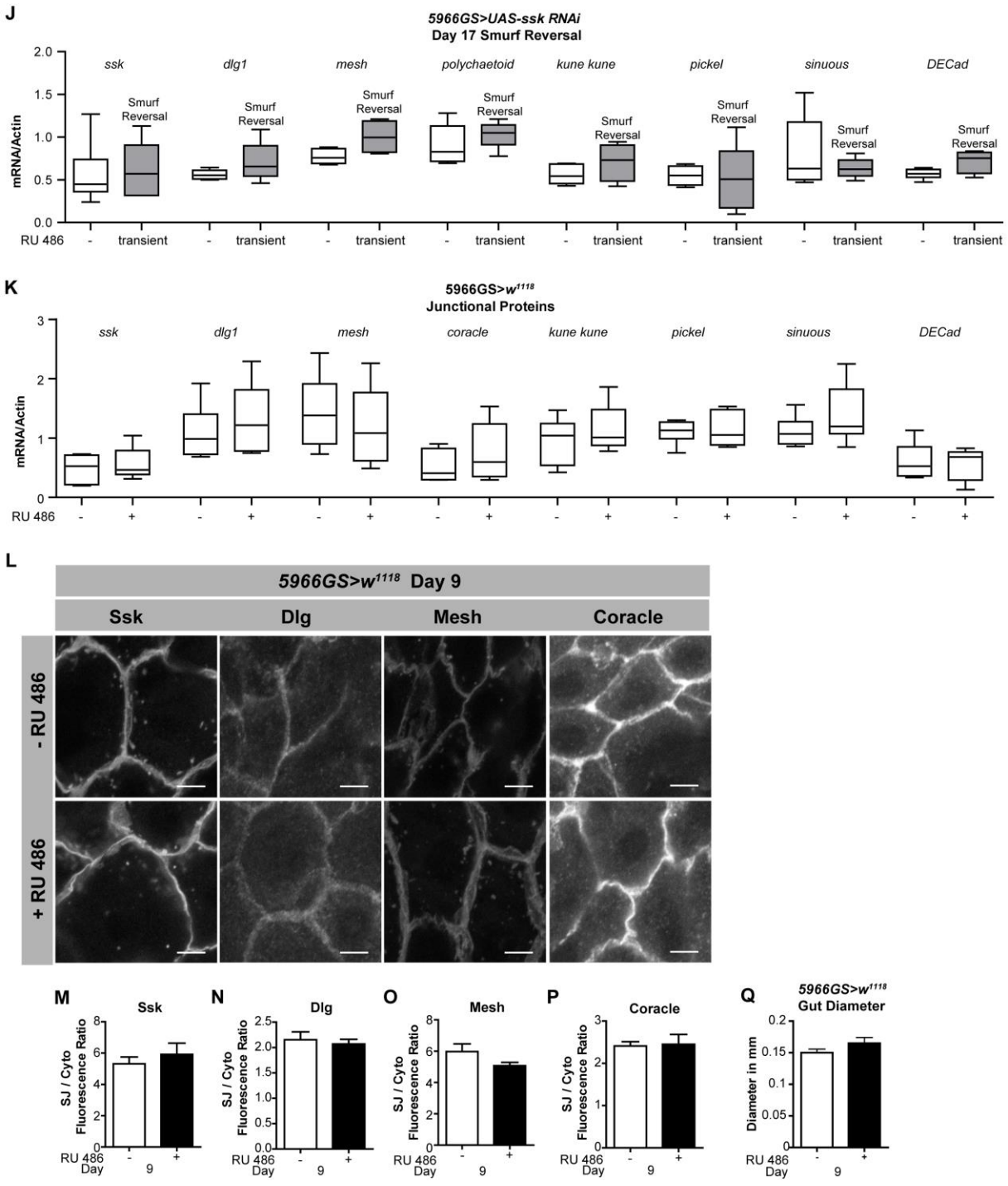

Figure S3. Loss of intestinal Ssk leads to gut distention and altered SJs. Related to Figure 3

(A) SJ protein localization in *5966GS>UAS-ssk RNAi* female flies on day 9 with or without RU486-mediated transgene induction from day 3 to day 9. Representative images for Dlg and Coracle. SJ protein mislocalization is observed in the presence of RU486. *Scale bar* is 20 μm.

(B) Junction protein gene expression assayed by qPCR from dissected intestines of *5966GS>UAS-ssk RNAi* female flies on day 9 with or without RU486-mediated transgene induction from day 3 to day 9. n = 6 replicates of five intestines. *ssk, snakeskin; dlg1, discs large 1; mesh; polychaetoid; kune-kune; pickle; sinuous, sinu; DeCad, Drosophila E-Cadherin.*

(C-H) Junction protein gene expression assayed by qPCR from dissected intestines in Smurf and non-Smurf *5966GS>UAS-ssk RNAi* female flies on day 9 with or without RU486-mediated transgene induction from day 3 to day 9. n = 6 replicates of five intestines. *dlg1, discs large 1; polychaetoid; kune-kune; pickle; sinuous, sinu; DeCad, Drosophila E-Cadherin.*

(I) Junction protein gene expression assayed by qPCR from dissected intestines of *5966GS>UAS-ssk RNAi* female flies on day 14 with or without RU486-mediated transgene induction from day 3 to day 14. n = 6 replicates of five intestines. *ssk, snakeskin; dlg1, discs large 1; polychaetoid; kune-kune; pickle; sinuous, sinu; DeCad, Drosophila E-Cadherin.*

(J) Reversal of junction protein gene expression assayed by qPCR from dissected intestines of *5966GS>UAS-ssk RNAi* female flies at 9 days of age with or without RU486-mediated transgene induction from day 3 until day 10, when all of the induced flies become Smurfs, then moved to food lacking RU486 for 7 days and assayed on day 17. n = 6 replicates of five intestines. *ssk, snakeskin; dlg1, discs large 1; mesh; polychaetoid; kune-kune; pickle; sinuous, sinu; DeCad, Drosophila E-Cadherin.*

(K) Junction protein gene expression assayed by qPCR from dissected intestines of *5966GS>w^{1118}* female flies on day 9 with or without RU486-mediated transgene induction from day 3 to day 9. n = 6 replicates of five intestines. *ssk, Snakeskin; dlg1, discs large 1; mesh; coracle; kune-kune; pickle; sinuous, sinu; DeCad, Drosophila E-Cadherin.*

(L) SJ protein localization for Ssk, Dlg, Mesh and Coracle in ECs from dissected intestines of *5966GS>w^{1118}* female flies on day 9 with or without RU486-mediated transgene induction from day 3 to day 9. No difference in SJ protein mis-localization is observed. n>13 midguts per condition; n=10 ECs were observed per midgut; s*cale bar* is 5 μm.

(M-P) SJ/Cytoplasm fluorescence ratios for Ssk, Dlg, Mesh and Coracle. There is no significant difference; two-tailed unpaired Student's t-test.

(Q) Posterior midgut diameter in mm from dissected intestines of *5966GS>w^{1118}* female flies on day 9 with or without RU486-mediated transgene induction from day 3 to day 9. No difference in midgut diameters are observed, two-tailed unpaired Student's t-test; n>13 midguts per condition.

Boxplots display the first and third quartile, with the horizontal bar at the median and whiskers showing the most extreme data point, which is no more than 1.5 times the interquartile range from the box. Error bars on bar graphs depict mean ± SEM. *$p < 0.05$; **$p < 0.01$; ***$p < 0.001$; Wilcoxon test unless otherwise stated.

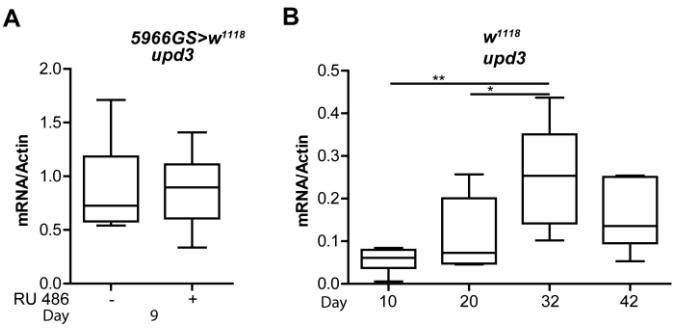

Figure S4. Loss of intestinal Ssk leads to intestinal stem cell dysfunction. Related to Figure 4

(A) *upd3* gene expression assayed by qPCR from dissected intestines in *5966GS> w^{1118}* female flies on day 9 with or without RU486-mediated transgene induction from day 3 to day 9. n = 6 replicates of five intestines.

(B) *upd3* gene expression assayed by qPCR from dissected intestines of w^{1118} non-Smurf female flies at 10, 20, 32, and 42 days of age. n = 6 replicates of five intestines.

Boxplots display the first and third quartile, with the horizontal bar at the median and whiskers showing the most extreme data point, which is no more than 1.5 times the interquartile range from the box. *p < 0.05; **p < 0.01; Wilcoxon test.

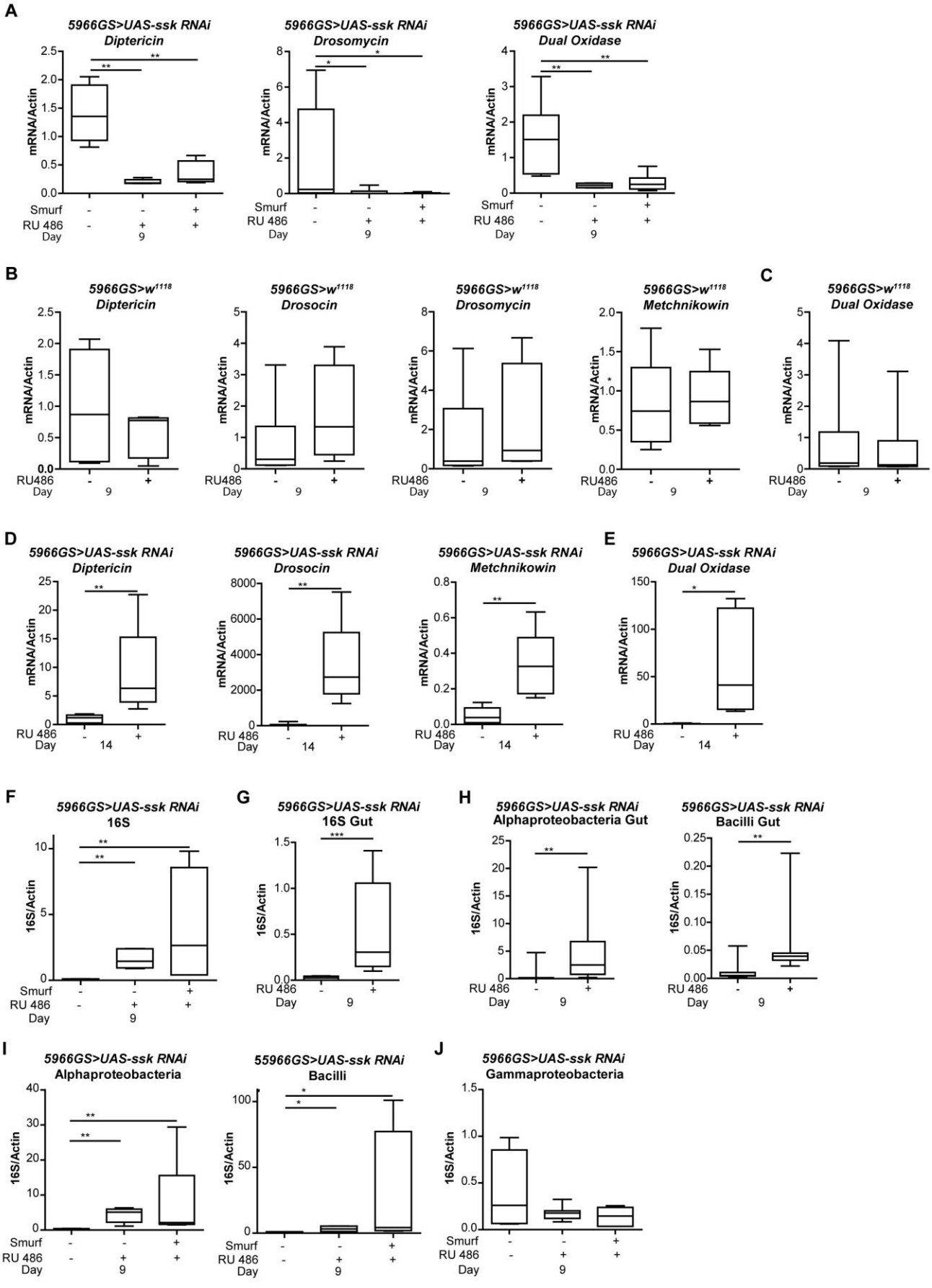
A
5966GS>UAS-ssk RNAi
Diptericin
5966GS>UAS-ssk RNAi
Drosomycin
5966GS>UAS-ssk RNAi
Dual Oxidase
mRNA/Actin
Smurf
RU 486
Day
B
5966GS>w1118
Diptericin
5966GS>w1118
Drosocin
5966GS>w1118
Drosomycin
5966GS>w1118
Metchnikowin
C
5966GS>w1118
Dual Oxidase
D
5966GS>UAS-ssk RNAi
Diptericin
5966GS>UAS-ssk RNAi
Drosocin
5966GS>UAS-ssk RNAi
Metchnikowin
E
5966GS>UAS-ssk RNAi
Dual Oxidase
F
5966GS>UAS-ssk RNAi
16S
16S/Actin
G
5966GS>UAS-ssk RNAi
16S Gut
H
5966GS>UAS-ssk RNAi
Alphaproteobacteria Gut
5966GS>UAS-ssk RNAi
Bacilli Gut
I
5966GS>UAS-ssk RNAi
Alphaproteobacteria
55966GS>UAS-ssk RNAi
Bacilli
J
5966GS>UAS-ssk RNAi
Gammaproteobacteria

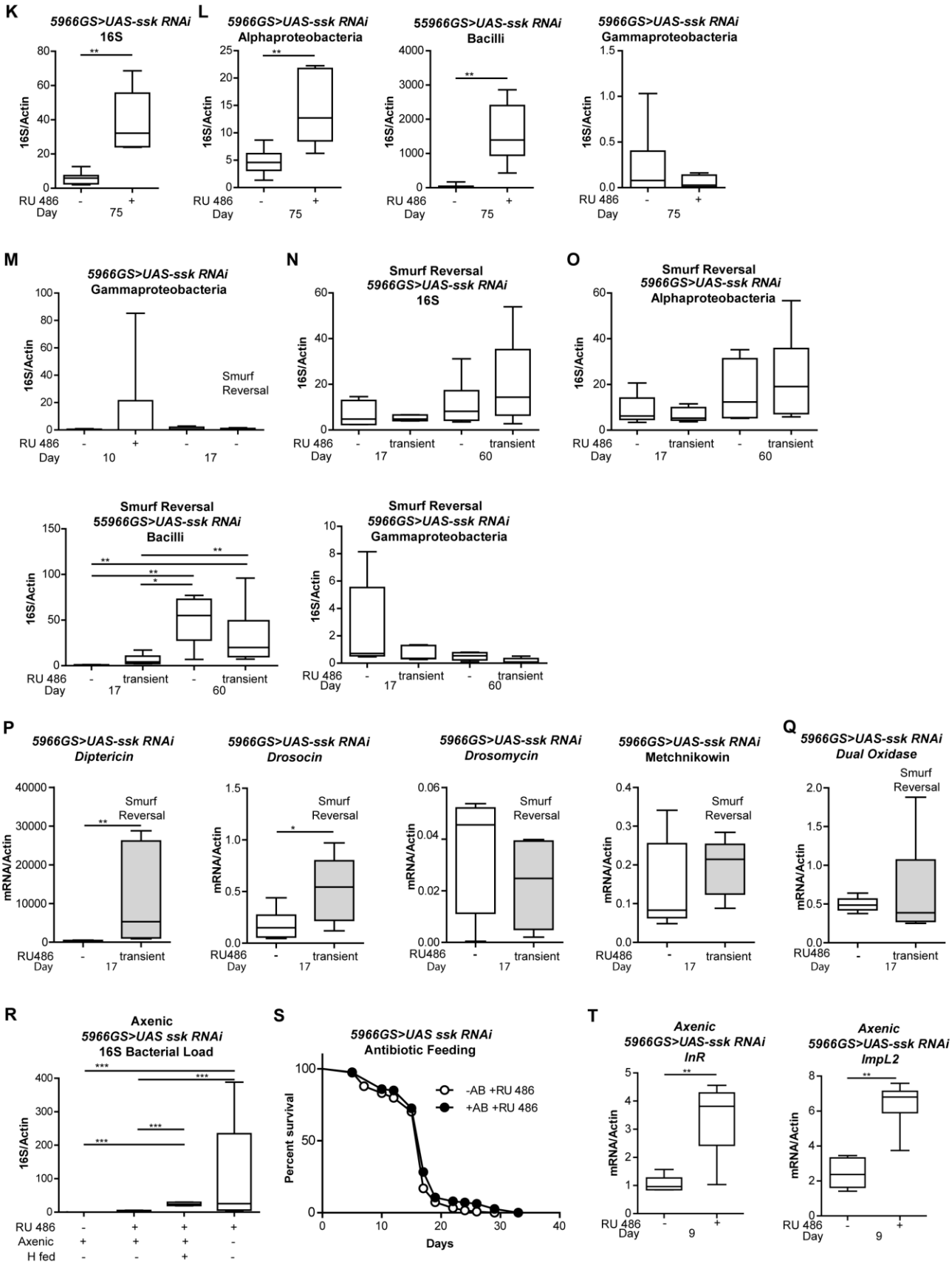
K
5966GS>UAS-ssk RNAi
16S
16S/Actin
RU 486
Day
75
L
5966GS>UAS-ssk RNAi
Alphaproteobacteria
55966GS>UAS-ssk RNAi
Bacilli
5966GS>UAS-ssk RNAi
Gammaproteobacteria
M
5966GS>UAS-ssk RNAi
Gammaproteobacteria
Smurf
Reversal
10
17
N
Smurf Reversal
5966GS>UAS-ssk RNAi
16S
transient
60
O
Smurf Reversal
5966GS>UAS-ssk RNAi
Alphaproteobacteria
Smurf Reversal
55966GS>UAS-ssk RNAi
Bacilli
Smurf Reversal
5966GS>UAS-ssk RNAi
Gammaproteobacteria
P
5966GS>UAS-ssk RNAi
Diptericin
Drosocin
Drosomycin
Metchnikowin
mRNA/Actin
RU486
Q
5966GS>UAS-ssk RNAi
Dual Oxidase
R
Axenic
5966GS>UAS ssk RNAi
16S Bacterial Load
Axenic
H fed
S
5966GS>UAS ssk RNAi
Antibiotic Feeding
-AB +RU 486
+AB +RU 486
Percent survival
Days
T
Axenic
5966GS>UAS-ssk RNAi
InR
ImpL2
9

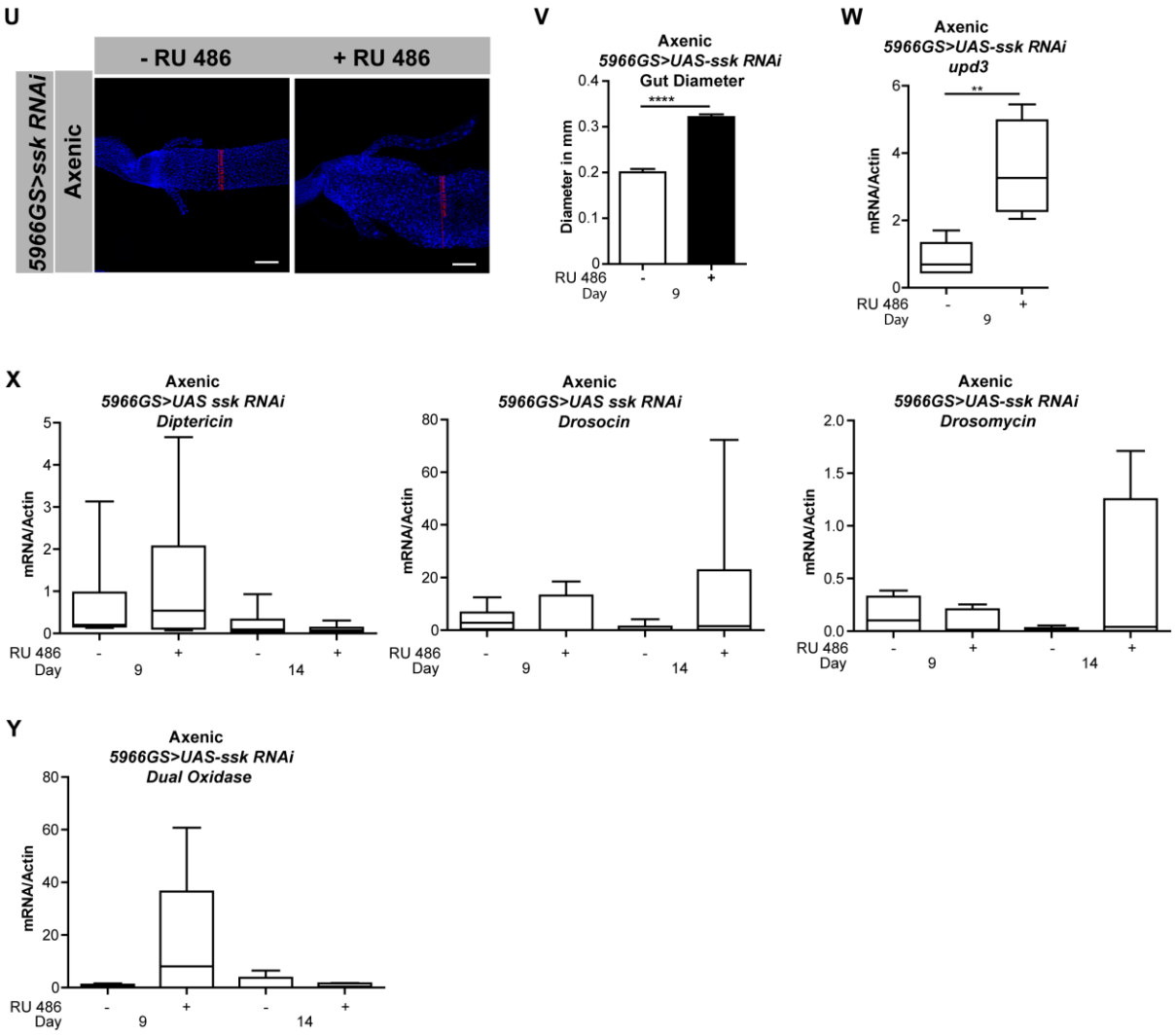

Figure S5. Loss of intestinal Ssk leads to reversible microbial dysbiosis. Related to Figure 5

(A) Antimicrobial peptide and *Dual Oxidase* gene expression assayed by qPCR from dissected intestines in Smurf and non-Smurf *5966GS>UAS-ssk RNAi* female flies on day 9 with or without RU486-mediated transgene induction from day 3 to day 9. *Diptericin, Drosomycin*; n = 6 replicates of five intestines.

(B and C) Antimicrobial peptide and *Dual Oxidase* gene expression assayed by qPCR from dissected intestines in *5966GS>w^{1118}* female flies on day 9 with or without RU486-mediated transgene induction from day 3 to day 9. There is no significant difference. *Diptericin, Drosocin, Drosomycin, Metchnikowin*; n = 6 replicates of five intestines.

(D and E) Antimicrobial peptide and *Dual Oxidase* gene expression assayed by qPCR from dissected intestines in *5966GS>UAS-ssk RNAi* female flies on day 14 with or without RU486-mediated transgene induction from day 3 to day 14. *Diptericin, Drosocin, Metchnikowin*; n = 6 replicates of five intestines.

(F) Bacterial levels assayed by qPCR of the 16S rRNA gene with universal primers in Smurf and non-Smurf *5966GS>UAS-ssk RNAi* female flies at 9 days of age with or without RU486-mediated transgene induction from day 3 to day 9. n = 6 replicates of 5 flies.

(G) Gut bacterial levels assayed by qPCR of the 16S rRNA gene from dissected intestines with universal primers in *5966GS>UAS-ssk RNAi* female flies at 9 days of age with or without RU486-mediated transgene induction from day 3 to day 9. n = 6 replicates of 5 flies.

(H) Gut bacterial levels assayed by qPCR of the 16S rRNA gene from dissected intestines by taxon-specific qPCR of the 16S rRNA gene in *5966GS>UAS-ssk RNAi* female flies at 9 days of age with or without RU486-mediated transgene induction from day 3 to day 9. Alphaproteobacteria, Bacilli; n = 6 replicates of 5 flies.

(I and J) Bacterial levels assayed by taxon-specific qPCR of the 16S rRNA gene in Smurf and non-Smurf *5966GS>UAS-ssk RNAi* female flies at 9 days of age with or without RU486-mediated transgene induction from day 3 to day 9. Alphaproteobacteria, Bacilli, Gammaproteobacteria; n = 6 replicates of 5 flies.

(K) Bacterial levels assayed by qPCR of 16S with universal primers in *5966GS>UAS-ssk RNAi* female flies at 75 days of age with or without RU486-mediated transgene induction from day 69 to day 75. n = 6 replicates of 5 flies.

(L) Bacterial levels assayed by taxon-specific qPCR of the 16S rRNA gene in *5966GS>UAS-ssk RNAi* female flies at 75 days of age with or without RU486-mediated transgene induction from day 69 to day 75. Alphaproteobacteria, Bacilli, Gammaproteobacteria; n = 6 replicates of 5 flies.

(M) Reversal of bacterial levels assayed by taxon-specific qPCR of the 16S rRNA gene in *5966GS>UAS-ssk RNAi* female flies at 9 days of age with or without RU486-mediated transgene induction from day 3 to day 10, when all induced flies become Smurfs, then removed from RU486-mediated induction for 7 more days until day 17, where flies were assayed to now be non-Smurfs. Gammaproteobacteria; n = 6 replicates of 5 flies per replicate.

(N) Maintenance of reversal of bacterial levels assayed by qPCR of the 16S rRNA gene with universal primers in *5966GS>UAS-ssk RNAi* female flies at 17 and 60 days of age with or without RU486-mediated transgene induction from day 3 to day 10, when all induced flies become Smurf, then removed from RU486-mediated induction for 7 more days until day 17, where flies were assayed to now be non-Smurfs, then were aged until day 60 on food lacking RU486. n = 6 replicates of 5 flies per replicate.

(O) Maintenance of reversal of bacterial levels assayed by taxon-specific qPCR of the 16S rRNA gene in *5966GS>UAS-ssk RNAi* female flies at 17 and 60 days of age with or without RU486-mediated transgene induction from day 3 to day 10, when all induced flies become Smurfs, then removed from RU486-mediated induction for 7 more days until day 17, where flies were assayed to now be non-Smurfs, then were aged until day 60 on food lacking RU486. Alphaproteobacteria, Bacilli, Gammaproteobacteria; n = 6 replicates of 5 flies per replicate.

(P and Q) Reversal of antimicrobial peptide and *Dual Oxidase* gene expression assayed by qPCR from dissected intestines of *5966GS>UAS-ssk RNAi* female flies at 9 days of age with or without RU486-mediated transgene induction from day 3 until day 10, when all of the induced flies become Smurfs, then moved to food lacking RU486 for 7 days and assayed on day 17. *Diptericin, Drosocin, Drosomycin, Metchnikowin;* n = 6 replicates of five intestines.

(R) Bacterial levels assayed by qPCR of the 16S rRNA gene with universal primers in Smurf and non-Smurf *5966GS>UAS-ssk RNAi* female flies at 14 days of age with or without RU486-mediated transgene induction from day 3 to day 14 under Axenic conditions, standard conditions, or after embryonic homogenate feeding. n = 6 replicates of 5 flies.

(S) Survival curves of *5966GS>UAS-ssk RNAi* females with or without antibiotics during RU486-mediated transgene induction from day 3 onwards. There is no significant difference, log rank test; n > 173 flies/condition. Median lifespan 17 and 17 days, respectively.

(T) FOXO target gene expression assayed by qPCR from dissected intestines in Axenic *5966GS>UAS-ssk RNAi* female flies on day 9 with or without RU486-mediated transgene induction from day 3 to day 9. *Insulin-like Receptor, InR*; Ecdysone-inducible gene L2, *ImpL2*; n = 6 replicates of five intestines.

(U and V) Representative images (U) and quantification (V) of posterior midgut diameters in mm from dissected intestines of Axenic *5966GS>UAS-ssk RNAi* female flies on day 9 with or without RU486-mediated transgene induction from day 3 to day 9. A significant increase in the midgut diameter is observed, $p < .0001$; two-tailed unpaired Student's t-test; n>14 midguts per condition; *scale bar* is 50 μm.

(W) *upd3* gene expression assayed by qPCR from dissected intestines in Axenic *5966GS>UAS-ssk RNAi* female flies on day 9 with or without RU486-mediated transgene induction from day 3 to day 9. n = 6 replicates of five intestines.

(X and Y) Antimicrobial peptide and *Dual Oxidase* gene expression assayed by qPCR from *5966GS>UAS-ssk RNAi* female flies grown under Axenic conditions on day 9 or day 14 with or without RU486-mediated transgene induction from day 3 to day 14. There is no significant difference. *Diptericin, Drosocin, Drosomycin;* n = 6 replicates of five intestines.

Boxplots display the first and third quartile, with the horizontal bar at the median and whiskers showing the most extreme data point, which is no more than 1.5 times the interquartile range from the box. Error bars on bar graphs depict mean ± SEM. *$p < 0.05$; **$p < 0.01$; ***$p < 0.001$; ****$p < 0.0001$; Wilcoxon test unless otherwise stated.

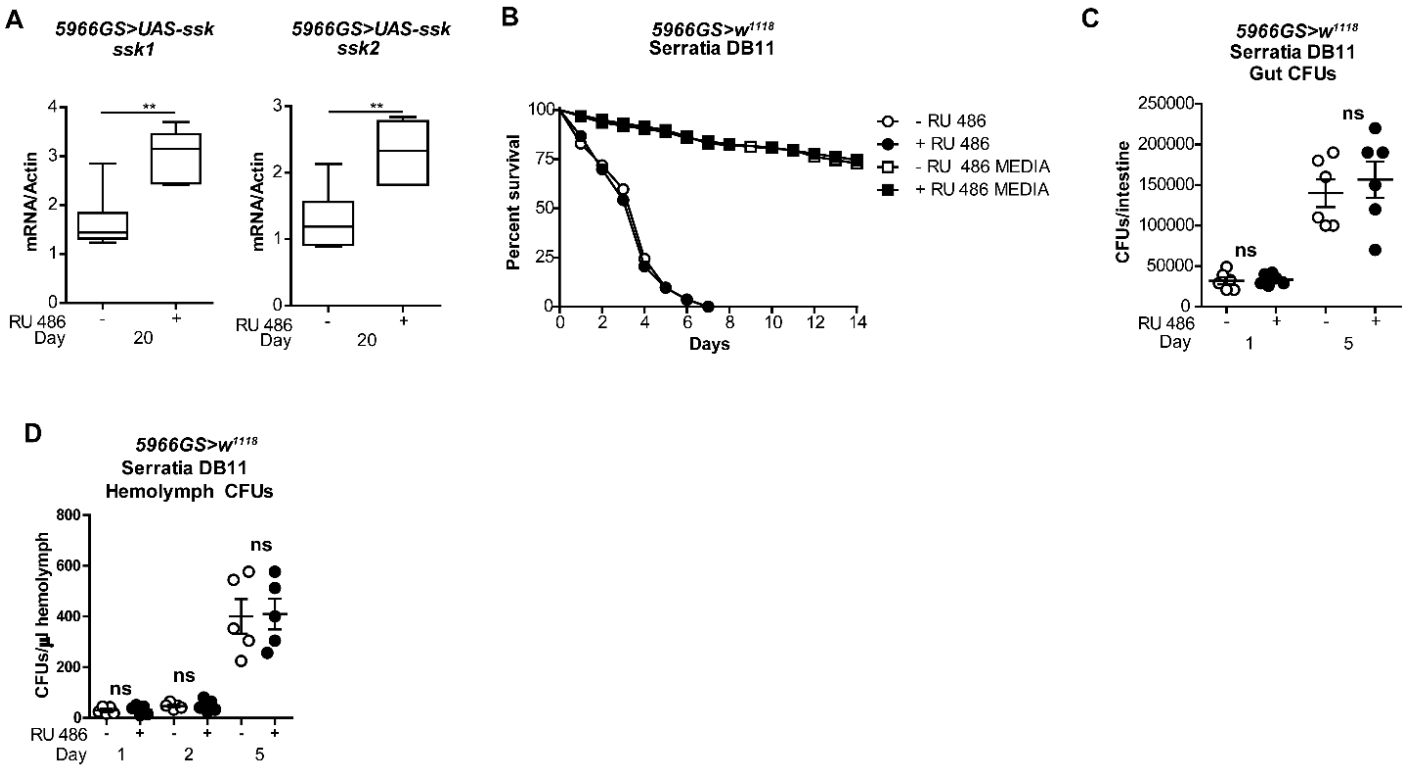

Figure S6. Intestinal Ssk reduces bacterial translocation and improves survival upon oral infection with pathogenic bacteria. Related to Figure 6

(A) *ssk* gene expression assayed by qPCR utilizing two different sets of primers: *ssk1* and ssk2, from dissected intestines of *5966GS > UAS-ssk* female flies at 20 days of age with or without RU486-mediated transgene induction from day 3 to day 20. Boxplots display the first and third quartile, with the horizontal bar at the median and whiskers showing the most extreme data point, which is no more than 1.5 times the interquartile range from the box. **p < 0.01; Wilcoxon test; n = 6 replicates of five intestines.

(B) Survival curves of *5966GS>w^{1118}* females with or without RU486 from day 3 until day 20, then Db11 bacteria were fed to the flies and survival plotted. There is no significant difference, log rank test; n > 82 flies/condition. Median survival 4 days.

(C) Colony-forming Units (CFUs) from dissected midguts of *5966GS>w^{1118}* females with or without RU486-mediated transgene induction from day 3 until day 20. Db11 bacteria were fed to the flies and the guts of infected flies were dissected and crushed, and dilutions of the extracts were plated on LB agar containing the appropriate antibiotics, on days specified, following Db11 infection. There is no significant difference; one-way ANOVA/Tukey's multiple comparisons test. Error bars depict mean ± SEM.

(D) Colony-forming Units (CFUs) from the hemolymph of *5966GS>w^{1118}* females with or without RU486-mediated transgene induction from day 3 until day 20. Db11 bacteria were fed to the flies and the hemolymph from infected flies were collected and plated on LB agar containing the appropriate antibiotics, on days specified, following Db11 infection. There is no significant difference; one-way ANOVA/Tukey's multiple comparisons test. Error bars depict mean ± SEM.

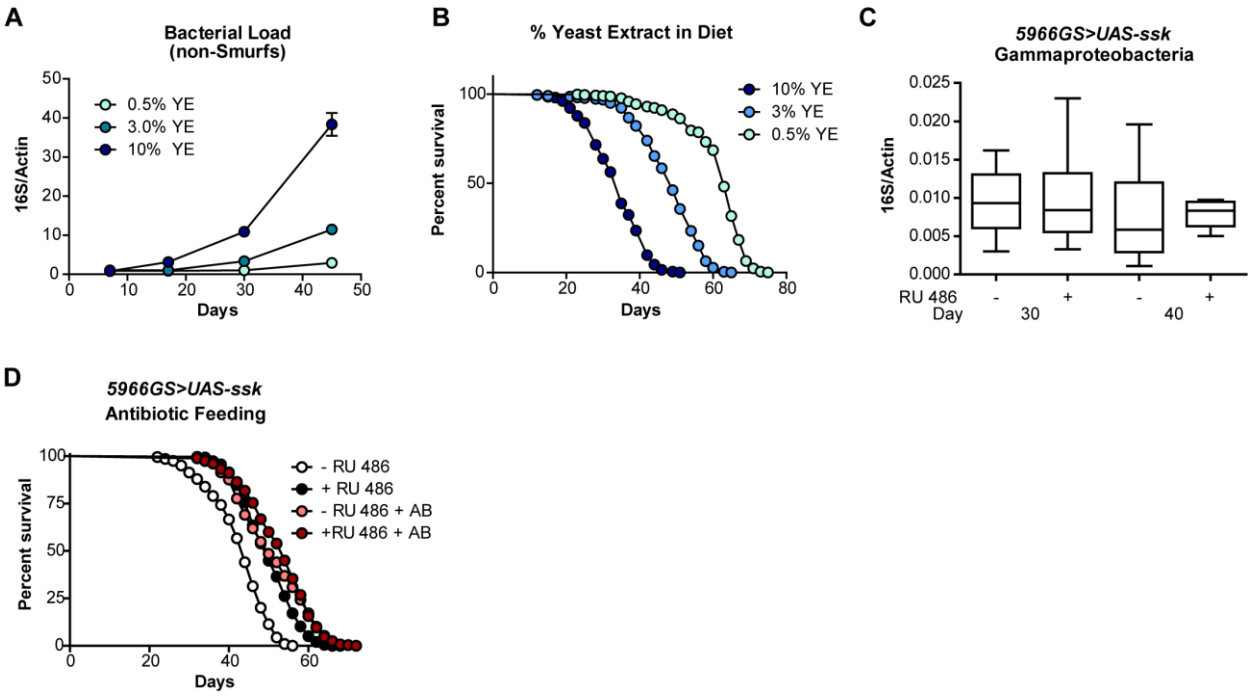

Figure S7. Ssk improves intestinal integrity during aging and prolongs lifespan. Related to Figure 7

A) Bacterial levels assayed by qPCR of the 16S rRNA gene in *Canton S* female flies at 7, 17, 30 and 45 days of age on media containing .5%, 3% or 10% yeast extract. $p < .001$ at day 45 between 10% YE and the other two YE concentrations; one-way ANOVA/Tukey's multiple comparisons test; n = 3 replicates of 30 flies.

(B) Survival curves of *Canton S* females on media containing .5%, 3% or 10% yeast extract. $p < .0001$ between each YE concentration, log rank test; n > 204 flies/condition. Median lifespan 35, 49, and 63 days, respectively.

(C) Bacterial levels assayed by taxon-specific qPCR of the 16S Gammaproteobacteria rRNA gene in *5966GS>UAS-ssk* female flies at 30 and 40 days of age with or without RU486-mediated transgene induction from day 3 onward on rich media. n = 6 replicates of 5 flies.

(D) Survival curves of *5966GS>UAS-ssk* females with or without RU486-mediated transgene induction with or without antibiotics from day 3 onwards on rich media. $p < .0001$, log rank test; n > 268 flies/condition. Median lifespan 44, 50, 50, and 54 days, respectively.

Boxplots display the first and third quartile, with the horizontal bar at the median and whiskers showing the most extreme data point, which is no more than 1.5 times the interquartile range from the box. Wilcoxon test unless otherwise stated.

Transparent Methods

Fly culture and Lifespan
Genotypes used were the standard laboratory strain *w^{1118}*, *5966 GeneSwitch* and *Su(H)lacZ; esg:GFP,5966GAL4^{GS}*, and *UAS-ssk* and *UAS-ssk RNAi* provided by M Furuse. We also obtained a second RNAi-mediated knock down line from the VDRC: *UAS-ssk RNAi* (11906GD). Flies were cultured in a humidified, temperature-controlled incubator with 12h on/off light cycle at 25 °C, in vials containing standard cornmeal medium (1% agar, 3% brewer's yeast, 1.9% sucrose, 3.8% dextrose and 9.1% cornmeal; all concentrations given in wt/vol). Overexpression studies were also carried out using an additional diet (1% agar, 3% yeast extract, 1.9% sucrose, 3.8% dextrose and 9.1% cornmeal; all concentrations given in wt/vol), designated as rich media in figures because of the higher nutritional content. Three concentrations of yeast extract were utilized to compare changes in bacterial load with diet: (1% agar; .5%, 3%, or 10% yeast extract; 1.9% sucrose; 3.8% dextrose; and 9.1% cornmeal; all concentrations given in wt/vol). Adult animals were collected under light nitrogen induced anesthesia, housed at a density of 27-32 flies per vial and flipped to fresh vials and scored for death every 2-3 days throughout adult life. RU486 (Cayman Chemical Company) was dissolved in ethanol and mixed into the media when preparing food vials.

RU486 doses used were 25 ug/ml final concentration and control food had ethanol alone, the volume of ethanol in each case was kept the same. Antibiotic treatment was conducted as described previously (Brummel et al., 2004). In every experiment, regardless of the conditions used, control and experimental animals are always transferred to fresh food at the same time-points. This provides an important control for bacterial growth in the food throughout these experiments.

Smurf and Smurf Reversal Assays
The Smurf assay was conducted as previously described (Rera et al., 2012), except that flies were kept on the blue food for a 24 hour period before being scored. New Smurfs were collected and removed from the blue dye. For reversal assays, after 7 days, flies were once again placed in vials with blue dye for 24 hours and the number of Smurf flies determined again.

Generation of axenic and re-associated flies
To generate axenic (germ-free) flies, embryos were treated by bleach and ethanol as described previously (Brummel et al., 2004). Briefly, <12-h-old embryos were dechorionated in 3% sodium hypochlorite (50% v/v regular bleach) for 20 min, rinsed in 70% ethanol for 5 min, and then washed three times with 1× PBS + 0.01% Triton X-100. Axenic embryos were transferred to autoclaved medium (50 embryos/vial) in a laminar flow cabinet. Axenic conditions were confirmed by quantitative PCR of the 16S rRNA gene from whole fly samples (see below) or plating the fly homogenate on MRS agar. To generate flies associated with microbes as embryos, whole fly homogenate (10 fly equivalent: 600 μL of conventionally reared fly homogenate glycerol stock/bottle) was added to medium containing axenic embryos.

Preparation of fly homogenate for re-association
Conventionally reared adult flies were surface sterilized by 70% ethanol prior to homogenization to ensure only internal microbes were present in the homogenate. Surface sterile flies were homogenized with a motor pestle in 1.5mL tube with 200 μL of sterile PBS (50 flies/tube). Homogenates were then pooled and sterile PBS added to adjust to one fly equivalent in 50 μL PBS. For storage 1/5 volume of 80% sterile glycerol was added and aliquots were stored at -80º C until use.

Starvation Resistance
Starvation assays were performed with mated female UAS-ssk RNAi knockdown flies crossed to 5966 Geneswitch-Gal4. 3-day-old adult flies were fed on vials containing 25 ug/mL of RU486 for 5 days at a density of 27-32 flies per vial. For agar starvation, flies were maintained on water only medium (1% agar in ddH2O wt/wt) that did not contain RU486 in a 25°C incubator with 12-hour light-dark cycles. Survival was scored multiple times per day.

Triacylglyceride Assay
Lipids were extracted from whole flies in a chloroform:methanol:water solution (2:5:1 by volumes) and nonpolar lipids were separated on thin layer chromatography plates (Analtech, Newark, DE, USA) with a n-hexane:diethylether:glacial acetic acid solution (70:30:1 by volumes). Plates were air-dried, stained (0.2% Amido

Black 10B in 1M NaCl), and lipid bands were quantified by photo densitometry using ImageJ as described (Rera et al., 2011).

Fluorescence Microscopy and Antibody Staining
Mated female flies of the appropriate age and background were sorted for Smurf status. Posterior midguts were dissected into ice-cold PBS/4% formaldehyde and incubated for 1hr in fixative at room temperature. Samples were then washed three times, for 10 min each, in PBT (PBS containing 0.5%Triton X-100), 10 min in Na-deoxycholate (0.3%) in PBT (PBS with 0.3%Triton X-100), and incubated in block (PBT-0.5% bovine serum albumin) for 30 min. Samples were immunostained with primary antibodies overnight at 4°C, washed 4 × 5 min at RT in PBT, incubated with secondary antibodies at RT for 2 h, washed three times with PBT and mounted in Vecta-Shield/DAPI (Vector Laboratories, H-1200).

The following antibodies were obtained from the Developmental Studies Hybridoma Bank, developed under the auspices of the NICHD and maintained by The University of Iowa, Department of Biology, Iowa City, IA 52242. Discs large (mouse, 1:20, 4F3) and Coracle (mouse, 1:20, C615.16). GFP (rabbit, 1:3,000, Molecular Probes A-11122); GFP (mouse, 1:200, Molecular Probes A-11120); GFP (chicken, 1:500, Aves Labs GFP-1010); Phospho-histone3 (rabbit, 1:200, Millipore 06-570). Snakeskin (rabbit, 1:1000) and Mesh (rabbit, 1:1000) (gifts from M. Furuse).

Images were acquired on a Zeiss LSM710 inverted confocal microscope, and on a Zeiss Axio Observer Z1 and processed with Fiji/ImageJ and Zen from Zeiss.

Septate Junction Fluorescence Quantification
To measure and quantify the possible differences, SJ fluorescence intensity in posterior midgut ECs, ×100 + ×3 of digital magnification confocal *z*-stack maximum projections at the level of the SJ were generated using Zen 2 pro Blue software edition (Zeiss). SJ fluorescence intensity were measured using a mask of 25.5 pixels in diameter. Then cytoplasm fluorescence intensity was calculated using the same mask. Average fluorescence intensity at the membrane was divided by the cytoplasmic average intensity. Between 3 to 7 measurements were taken per picture and a minimum of 20 posterior midguts were analysed per experimental condition.

Gut Diameter Calculation
To measure variations in gut diameter single z-stack images were taken at 20x magnification in a Zeiss Axio Observer Z1 microscope, and measured using Zen 2 pro Blue software edition (Zeiss). Diameter was calculated for each midgut at the same distance from the pylorus.

Cell Division Quantification Using CellProfiler
For statistical significance four images were taken as *z*-stacks with a typical slice thickness of 750 nm per posterior midgut; two on each side (top and bottom); from contiguous field of view (fov), starting at 1 fov from the pylorus (using a minimum of 20 guts). The images were then processed using the CellProfiler pipeline (Carpenter et al., 2006) developed in the Jones laboratory. ISC number and mitotic events were obtained from esg:GFP/total cell and PH3/total cell ratios respectively. Average ratios from the four images corresponding to a single gut were used in subsequent statistical analyses.

Genomic DNA Isolation to Assess Bacterial Levels
The reported effects of husbandry practices on *Drosophila* bacterial loads (Blum et al., 2013) were controlled for by keeping bacterial sample collection consistent relative to new food transfer and by the collection of non-Smurf controls from the same vials as Smurf individuals. Genomic DNA was extracted using the PowerSoil DNA isolation kit (MoBio). All flies were surface sterilized prior to sample preparation. To ensure consistent homogenization, whole fly samples were pre-homogenized in 150µL of solution from the PowerSoil bead tube using a motor pestle. This homogenate was then returned to the bead tube and the manufacturers protocol was followed. For intestinal samples, flies were surface sterilized in small groups and then dissected over ice, in sterile PBS and with sterile equipment. The dissection surface was swabbed with 75% ethanol between each sample. Intestinal dissections included all but the anterior foregut, from the point at which the crop diverges, and including the crop, to the rectal papilla. Care was taken to keep the full length of the gut intact to prevent loss of lumen contents. Dissected intestines were stored in sterile eppendorf tubes at -80ºC prior to DNA extraction and were then prehomogenized as described above.

Quantitative PCR
DNA samples for qPCR of the 16S ribosomal RNA gene were prepared as described above.
RNA extractions, for gene expression analysis, were carried out in TRIzol (Invitrogen) following the manufacturer's directions. Intestinal dissections for RNA extraction were as described for DNA isolation but without the sterilization steps. cDNA synthesis was carried out using the First Strand cDNA Synthesis Kit from Fermentas. PCR was performed with Power SYBR Green master mix (Applied Biosystems) on an Applied Biosystems 7300 Real Time PCR system. Cycling conditions were as follows: 95ºC for10 minutes; 95ºC for 15s then 60ºC for 60s, cycled 40 times. All calculated gene expression values were normalized to the value of the loading control gene, Actin5C.

The primer sequences used to assess gene expression in this study were as follows:
Act5C_L –TTGTCTGGGCAAGAGGATCAG, Act5C_ R – ACCACTCGCACTTGCACTTTC;
Dro_L –CCATCGAGGATCACCTGACT, Dro_R – CTTTAGGCGGGCAGAATG;
Drs_L –GTACTTGTTCGCCCTCTTCG, Drs_R – CTTGCACACACGACGACAG;
Dpt_L –ACCGCAGTACCCACTCAATC, Dpt_R – CCCAAGTGCTGTCCATATCC;
Mtk_L –TCTTGGAGCGATTTTTCTGG, Mtk_R – TCTGCCAGCACTGATGTAGC;
Duox_L –GGGAGTCTTATGGACTGAAAC, Duox_ R – GTACGCCTCCTTCAGCATGT;
upd3_L –GCAAGAAACGCCAAAGGA, upd3_R – CTTGTCCGCATTGGTGGT;
DEcad_L –GACGAATCCATGTCGGAAAA, DEcad_R – TCACTGGCGCTGATAGTCAT;
delta_L -AGTGGGGTGGGTGTAGCTTT, delta_R – GCTGTTGCTGCCAGTTTTG;
Notch_L –GAATTTGCCAAACACCGTTC, Notch_R – ACCGACACTTGTGCAGGAA;
pck_L –GCTCTCGCTTACCATCATCC, pck_R – TACGGCCAAAAACATGAACA;
Kune_L –AGGTTGTGGGCTCTGTTTTC, Kune_R – ATCCCGAGAATCTCCTTTGG;
sinu_L –CATTGAATTGCATAAACTTCAGCTA, sinu_R – GCGGAGTTTCGCTTACCTT;
pyd_L –TGAATCGAGAGGCAACTTCTT, pyd_R – TTCTCGCGGGACAGACTC;
dlg1_L –AGAGTCGCGATGAGAAGAATG, dlg1_R – GCTGGTGCTGCTCACAACT.
Mesh_L–AGCCCGATCAATACTCAGGA, Mesh_R – CCATATACCAGGCCAGAGGA
Ssk1_L– CACTGGATGCCACACCATT, Ssk1_R–TGGTGTCGCACAGCTCTC
Ssk2_L–TCAAGGCCCTGAAGCTGA, Ssk2_R–GCTCTTCTCCTCGTTTAAGTTCC
InR_L–GCACCATTATAACCGGAACC, InR_R–TTAATTCATCCATGAGGTGAG
Imp2L_L–GCCGATACCTTCGTGTATCC, Imp2L_R– TTTCCGTCGTCAATCCAATAG

Universal primers for the 16S ribosomal RNA gene were against variable regions 1 (V1F) and 2 (V2R) (Claesson et al., 2010), as previously published (Clark et al., 2015). Taxon-specific 16S primers (Clark et al., 2015) were as follows:
Bacilli_F – CGACCTGAGAGGGTAATCGGC, Bacilli_R – GTAGTTAGCCGTGGCTTTCTGG;
Alpha_F – CCAGGGCTTGAATGTAGAGGC, Alpha_R – CCTTGCGGTTCGCTCACCGGC;
Gamma_F – GGTAGCTAATACCGCATAACG, Gamma_ R – TCTCAGTTCCAGTGTGGCTGG.

Intestinal Infection
Oral infection experiments were performed similarly to (Nehme et al., 2007) with some modifications. *Serratia marcescens* strain DB11 was grown in BHI (brain heart infusion) medium containing 100µg/ml of streptomycin at 37˚C to an optical density (OD) at 600nm of 1. Bacterial cultures were centrifuged and resuspended at a final concentration of OD600 0.3 in sterile *Drosophila* infection medium (3% yeast extract, 5% sucrose, and either 25µg/ml of RU486 or the same volume of ethanol vehicle for controls). Approximately 25 *Drosophila* of indicated age were placed in sterile vials containing Kim Wipes © saturated with bacterial solution, or infection medium only controls. Infections were maintained in an incubator at 29˚C at 60% humidity in a 12 hour Light:Dark cycle. Vials were scored for death daily, and vials were changed every two days.

Colony Forming Units Assay (CFUS)
Orally infected *Drosophila* of indicated age and time of infection were anesthetized by cold shock 4˚C. Flies were then washed three times in 70% ethanol. Followed by two washes in sterile PBS to remove bacteria present on the cuticle. For hemolymph CFUS, head hemolymph was extracted from flies using a 10µl pipette tip. Approximately 10 heads of the indicated condition were used per replicate to yield approximate 2 µl of hemolymph. Hemolymph was then serial diluted in PBS + 0.5% EDTA and plated on Luria Broth (LB) plates containing 100µg/ml of streptomycin. Plates were grown overnight at 37˚C and colonies were counted. For intestinal CFUS, five intestines

from flies of indicated condition were dissected in sterile PBS. Intestines lysates were ground up using a plastic pestle then serial diluted in sterile PBS and plated in Luria Broth (LB) plates containing 100µg/ml of streptomycin, followed by overnight growth and colony counting.

Electron Microscopy

Standard procedures for electron microscopic (EM) analysis were carried out as described in (Walker et al., 2006) with slight modifications. Dissected guts were fixed in 2% glutaraldehyde and 2% formaldehyde in 0.1 M sodium phosphate buffer (PB) containing 0.9% NaCl overnight at 4 °C. Guts were then post-fixed in 1% osmium tetroxide in PB, treated with 0.5% uranyl acetate, and dehydrated through a graded series of ethanol concentrations. After infiltration with Eponate 12 resin, the samples were embedded in fresh Eponate and polymerized overnight. Semi-thin sections (1.5 µm) were cut on an ultramicrotome and stained with toluidine blue. The midgut area of interest was identified from these sections. For EM, sections of 50 nm thickness were prepared from the identified area, placed on formvar coated copper grids and stained with uranyl acetate and Reynolds' lead citrate. The grids were examined using a JEOL 100CX transmission electron microscope at 60 kV (Electron Microscopy Facility, UCLA Brain Research Institute).

Statistics

The comparison of survival curves was done using the log-rank test as implemented in the Graphpad Prism software. Comparison of Smurf proportions per time point were carried out using one-way ANOVA/Bonferroni's multiple comparisons test with the error bars representing the standard error of the mean (SEM). SJ/cytoplasm fluorescence ratios for different SJ components were done using a Student's t-test with the error bars representing the SEM. The comparisons of gut diameters and infection CFUs analyzed with one-way ANOVA/Tukey's multiple comparisons test with the error bars representing the SEM range of those averages. All other data comparisons were tested for significant differences using the Wilcoxon-Mann-Whitney U test where sample sizes were greater than five, and a Student's t-test where sample sizes were fewer than five. The number of biological replicate samples is given in each figure legend. All statistical tests were implemented in Graph Pad Prism. All statistical tests are two-sided.

References

Blum, J.E., Fischer, C.N., Miles, J., and Handelsman, J. (2013). Frequent replenishment sustains the beneficial microbiome of Drosophila melanogaster. MBio *4*, e00860-00813.

Brummel, T., Ching, A., Seroude, L., Simon, A.F., and Benzer, S. (2004). Drosophila lifespan enhancement by exogenous bacteria. Proc Natl Acad Sci U S A *101*, 12974-12979.

Claesson, M.J., Wang, Q., O'Sullivan, O., Greene-Diniz, R., Cole, J.R., Ross, R.P., and O'Toole, P.W. (2010). Comparison of two next-generation sequencing technologies for resolving highly complex microbiota composition using tandem variable 16S rRNA gene regions. Nucleic Acids Res *38*, e200.

Clark, R.I., Salazar, A., Yamada, R., Fitz-Gibbon, S., Morselli, M., Alcaraz, J., Rana, A., Rera, M., Pellegrini, M., Ja, W.W., *et al.* (2015). Distinct Shifts in Microbiota Composition during Drosophila Aging Impair Intestinal Function and Drive Mortality. Cell Rep *12*, 1656-1667.

Nehme, N.T., Liegeois, S., Kele, B., Giammarinaro, P., Pradel, E., Hoffmann, J.A., Ewbank, J.J., and Ferrandon, D. (2007). A model of bacterial intestinal infections in Drosophila melanogaster. PLoS Pathog *3*, e173.

Rera, M., Bahadorani, S., Cho, J., Koehler, C.L., Ulgherait, M., Hur, J.H., Ansari, W.S., Lo, T., Jr., Jones, D.L., and Walker, D.W. (2011). Modulation of longevity and tissue homeostasis by the Drosophila PGC-1 homolog. Cell Metab *14*, 623-634.

Rera, M., Clark, R.I., and Walker, D.W. (2012). Intestinal barrier dysfunction links metabolic and inflammatory markers of aging to death in Drosophila. Proc Natl Acad Sci U S A *109*, 21528-21533.

Walker, D.W., Hajek, P., Muffat, J., Knoepfle, D., Cornelison, S., Attardi, G., and Benzer, S. (2006). Hypersensitivity to oxygen and shortened lifespan in a Drosophila mitochondrial complex II mutant. Proc Natl Acad Sci U S A *103*, 16382-16387.